




Palladium Nanoparticle-Induced Oxidative Stress, Endoplasmic Reticulum Stress, Apoptosis, and Immunomodulation Enhance the Biogenesis and Release of Exosome in Human Leukemia Monocytic Cells (THP-1)

This article was published in the following Dove Press journal:
International Journal of Nanomedicine

Sangiliyandi Gurunathan 
Min-Hee Kang 
Muniyandi Jeyaraj
Jin-Hoi Kim 

Department of Stem Cell and
Regenerative Biotechnology, Konkuk
University, Seoul, Korea

Background: Exosomes are endosome-derived nano-sized vesicles that have emerged as important mediators of intercellular communication and play significant roles in various diseases. However, their applications are rigorously restricted by the limited secretion competence of cells. Therefore, strategies to enhance the production and functions of exosomes are warranted. Studies have shown that nanomaterials can significantly enhance the effects of cells and exosomes in intercellular communication; however, how palladium nanoparticles (PdNPs) enhance exosome release in human leukemia monocytic cells (THP-1) remains unclear. Therefore, this study aimed to address the effect of PdNPs on exosome biogenesis and release in THP-1 cells.

Methods: Exosomes were isolated by ultracentrifugation and ExoQuick™ and characterized by dynamic light scattering, nanoparticle tracking analysis system, scanning electron microscopy, transmission electron microscopy, EXOCET™ assay, and fluorescence polarization. The expression levels of exosome markers were analyzed via quantitative reverse transcription-polymerase chain reaction and enzyme-linked immunosorbent assay.

Results: PdNP treatment enhanced the biogenesis and release of exosomes by inducing oxidative stress, endoplasmic reticulum stress, apoptosis, and immunomodulation. The exosomes were spherical in shape and had an average diameter of 50–80 nm. Exosome production was confirmed via total protein concentration, exosome counts, acetylcholinesterase activity, and neutral sphingomyelinase activity. The expression levels of TSG101, CD9, CD63, and CD81 were significantly higher in PdNP-treated cells than in control cells. Further, cytokine and chemokine levels were significantly higher in exosomes isolated from PdNP-treated THP-1 cells than in those isolated from control cells. THP-1 cells pre-treated with N-acetylcysteine or GW4869 showed significant decreases in PdNP-induced exosome biogenesis and release.

Conclusion: To our knowledge, this is the first study showing that PdNPs stimulate exosome biogenesis and release and simultaneously increase the levels of cytokines and chemokines by modulating various physiological processes. Our findings suggest a reasonable approach to improve the production of exosomes for various therapeutic applications.

Keywords: exosomes, biogenesis, human leukemia monocytic cells, palladium nanoparticles, oxidative stress, endoplasmic reticulum stress

Correspondence: Jin-Hoi Kim
Department of Stem Cell and
Regenerative Biotechnology, Konkuk
University, Seoul, 05029, Korea
Tel +82 2 450 3687
Fax +82 2 544 4645
Email jhkim541@konkuk.ac.kr

Introduction

Leukemia is a cancer of early blood-forming cells caused by a rise in the number of white blood cells. The exact causes of leukemia are not well known; however, some of these factors appear to be causative agents such as smoke, radiation, chemotherapy, genetic disorders, and age. Among all types of cancers, leukemia is estimated to account for approximately 3.5%.¹ Treatment for leukemia varies from person to person as well as with the type of leukemia; however, common methods are adopted, including chemotherapy, stem cell transplant, radiation therapy, targeted therapy, watchful waiting, and supportive therapy. Recently, exosome-based cancer therapy has gained immense attention owing to its unique properties such as non-toxicity, non-immunogenicity, robust delivery capacity, and targeting specificity. These features present exosomes as powerful nano-carriers for the delivery of anti-cancer drugs.

Extracellular vesicles (EVs) are a significant class of membrane-bound bodies that are involved in intercellular communication in various physiological and pathological processes. EVs are typically divided into three main categories based on biogenesis and size, which include exosomes, shed microvesicles and apoptotic bodies.^{2–4} Exosomes, a subset of EVs, are secreted by virtually all cells, including human leukemia monocytic (THP-1) cells, into bodily fluids. Exosomes play significant roles in trafficking macromolecules, including proteins, microRNAs, and long non-coding RNAs among cells, and regulating various cellular processes. They also serve as screening biomarkers and potential therapeutic targets in leukemia. Exosomes released from leukemia cells regulate drug resistance, immune dysfunction, and microenvironment manipulation.⁵ Exosomes are released by the fusion of multivesicular bodies with the plasma membrane and exhibit a cup-shaped morphology with characteristic markers such as tetraspanin proteins, including CD63, CD9, and CD81.^{6–8} Further, exosomes are carriers of cell-specific cargos of proteins, lipids, and genetic materials and all these cargoes transferred into neighboring or distant cells. Almost all types of cells release exosomes; however, the harbored cargoes differ from each other in terms of the functions of the parent cells and their current states.⁹

Exosomes are formed from late endosomes by inward budding of the limited multivesicular body (MVB) membrane. Invagination of late endosomal membranes results in the formation of intraluminal vesicles (ILVs) within

large MVBs and released into extracellular space.^{10,11} Several studies have shown that the formation of ILVs requires the endosomal sorting complex required for transport (ESCRT) function. The ESCRT mechanism is initiated by the recognition and sequestration of ubiquitinated proteins to specific domains of the endosomal membrane via ubiquitin binding subunits of ESCRT-0. The formation of ILVs is regulated by ESCRT complexes (0–III). In particular, the typical exosomal protein Alix, which is associated with several ESCRT (TSG101 and CHMP4) proteins, is involved in endosomal membrane budding and abscission, as well as exosomal cargo selection via interaction with syndecan.¹² Other pathways are involved in the biogenesis and release of exosomes in an ESCRT-independent manner, which seems to depend on raft-based microdomains, highly enriched in sphingomyelinases, from which ceramides are formed.¹³ Ceramides are known to induce lateral phase separation and coalescence of microdomains and also provide curvature of the endosomal membrane, thereby promoting domain-induced budding. Hence, a ceramide-dependent mechanism plays a critical role in exosome biogenesis.¹⁴ The critical components of exosomal proteins such as tetraspanins are involved in exosome biogenesis and protein loading, and tetraspanin-enriched microdomains (TEMs) are involved in the compartmentalization of receptors and signaling proteins in the plasma membrane.¹⁵

EV biogenesis and release is regulated by various factors such as cholesterol,¹⁶ cell detachment,¹⁷ cell type,¹⁸ media and concentration of serum in the media,¹⁹ Ca²⁺ ionophores,²⁰ hypoxia,²¹ and oxidative stress.²² Oxidative stress-induced autophagy promotes exosomes release.²³ Intracellular calcium concentration- and oxidative stress-induced Hb oxidation are major mechanisms involved in EV formation.²⁴ Liposomes, such as neutral, cationic-bare, or PEGylated liposomes, increase the release of exosomes in cancer cell lines.²⁵ Serum removal induces cellular stress,²⁶ alter EV number,^{27–29} activity,^{26,28,29} and composition,²⁹ as well as surface²⁸ and intra-vesicular proteins.²⁹ Further, serum deprivation improves exosome activity and alters the lipid and protein compositions of mesenchymal stem cells.³⁰ Thermal, oxidative stress, and hypoxic conditions enhance exosome secretion from leukemia/lymphoma T/B-cell lines.^{31,32} Melphalan and/or bortezomib increases exosome release in multiple myeloma cells,^{33,34} and chemotherapeutic agents such as 5-fluorouracil, cisplatin, and doxorubicin have been reported to induce

an increase in the amount of HSP70⁺ exosomes secreted from melanoma and colon cancer cell lines.³⁵

Considering the literature, environmental factors, culture media, serum, and other external factors significantly affect EV production and quantity; however, the impact of palladium nanoparticles (PdNPs) on exosome biogenesis pathways directly or indirectly remains elusive. In particular, PdNP-induced oxidative stress-elicited changes or release of exosomes has not yet been elucidated in THP-1 cells, which are valuable tools for investigating monocyte structure and function in both health and disease. THP-1 cells have a stable genetic background and have a reproducible treatment response.³⁶ Hence, in this study, we selected THP-1 cells as a model system to decipher the effect of PdNP-induced oxidative stress, endoplasmic reticulum stress, apoptosis, and immunomodulation on exosome biogenesis and release.

Materials and Methods

Synthesis and Characterization of PdNPs

PdNPs were prepared using nobiletin as previously described.³⁷ Nobiletin (5 mg) was suspended in 90 mL of sterile distilled water, mixed for 5 min, and then used in the synthesis of PdNPs. The nobiletin solution was combined with 10 mL of a 1-mM aqueous PdCl₂ solution and then incubated for 6 h at 60°C with constant stirring. Purification and characterization were carried out according to a previously described method.³⁸ Detailed methodology given as [Supplementary File](#).

Cell Culture Conditions and PdNPs Exposure

The THP-1 cell line was obtained from the American Type Culture Collection (ATCC; Manassas, VA, USA). THP-1 cells were cultured in RPMI-1640 cell culture medium supplemented with 10% FCS, 2 mM L-glutamine, 10 mM HEPES, 1 mM pyruvate, 100 U/mL penicillin, and 0.1 mg/mL streptomycin (Sigma-Aldrich). The cells were sub-cultured usually twice a week with 1×10^6 viable cells/mL and incubated at 37°C in a 5% CO₂ atmosphere. The medium was replaced the next day with 100-μL fresh media, and the cells were incubated for 24 h prior to PdNPs exposure. Experiments were performed in 96-, 24-, and 12-well plates and 100-mm cell culture dishes, as required. Cells were treated with various concentrations of PdNPs, CSP, or GW4869 or the required dose.

Cell Viability Assay and BrdU Cell Proliferation Assay

Cell viability was measured using the Cell Counting kit-8 (CCK-8; CK04-01, Dojindo Laboratories, Kumamoto, Japan). Briefly, THP-1 cells were plated in 96-well flat-bottom culture plates containing various concentrations of PdNPs (5.0–25.0 μM), CSP (5.0–25.0 μM), and GW4869 (5.0–25.0 μM), or PdNPs (15.0 μM), CSP (10.0 μM), and GW4869 (20 μM). After 24-h culture at 37°C in a humidified 5% CO₂ incubator, the CCK-8 solution (10.0 μL) was added to each well, and the plate was incubated for another 2 h at 37°C.

Assessment of Membrane Integrity and Cell Mortality Assay

The membrane integrity of THP-1 cells was evaluated using a lactate dehydrogenase (LDH) cytotoxicity detection kit. Briefly, the cells were exposed to various concentrations of PdNPs (15 μM), CSP (10 μM), or GW4869 (20 μM) for 24 h. Subsequently, 100 μL of cell-free supernatant from each well was transferred in triplicate into the wells of a 96-well plate, and 100 μL of the LDH reaction mixture was added to each well and intensity was determined using a microplate reader. Cell mortality was evaluated using the trypan blue assay, as described previously.³⁹

Determination of ROS, MDA, Nitric Oxide (NO), Carbonylated Protein Levels, Lipid Hydroperoxide, and 8-Isoprostane

ROS were estimated as described previously.⁴⁰ NO production was quantified spectrophotometrically using Griess reagent (Sigma-Aldrich).^{40,41} Carbonylated protein content was determined according to a previously described method.^{40,42} Lipid hydroperoxide and 8-isoprostane levels were also measured as previously described.^{38,43}

Measurement of Anti-Oxidative Marker Levels

THP-1 cells were treated with PdNPs (15 μM), CSP (10 μM), or GW4869 (20 μM) and incubated for 24 h. The expression levels of anti-oxidant markers such as glutathione (GSH), thioredoxin reductase (TRX), catalase (CAT), superoxide dismutase (SOD), glutathione peroxidase (GPx), and glutathione S-transferase (GST) were

determined as described previously⁴⁰ and per the assay kits manufacturer's instructions.

Mitochondrial Membrane Potential (MMP) and Measurement of Caspase-9/3 Activity

MMP was measured using the JC-1 cationic fluorescent indicator according to the manufacturer's instructions (Molecular Probes, Eugene, OR, USA). THP-1 cells were treated with PdNPs (15 μ M), CSP (10 μ M), or GW4869 (20 μ M) and incubated for 24 h, followed by treatment with 10 μ M JC-1 at 37°C for 15 min. Cells were then washed and resuspended in PBS, and fluorescence intensity was measured by measuring the ratio between J-aggregates in intact mitochondria fluorescence red with emission at 583 nm, and J-monomers in the cytoplasm fluorescence green with emission at 525 nm and an excitation wavelength of 488 nm. Mitochondrial membrane potential was expressed as the ratio of the fluorescence intensity of the JC-1 aggregates to that of the monomers. The caspase-9/3 activity was measured according to a previously described method.³⁸

Measurement of 4-Hydroxynonenal (HNE), 8-Oxo-7,8-Dihydro-2'-Deoxyguanosine (8-Oxo-dG), and 8-Oxo-G Levels

THP-1 cells were treated with PdNPs (15 μ M), CSP (10 μ M), or GW4869 (20 μ M) and incubated for 24 h. Afterward, 4-hydroxynonenal (HNE), 8-OHDG, and 8-OHG levels were determined as previously described^{38,40} and per the assay kits manufacturer's instructions (Trevigen, Gaithersburg, MD, USA).

Exosome Isolation via Ultracentrifugation

THP-1 cells were treated with PdNPs (15 μ M), CSP (10 μ M), or GW4869 (20 μ M) and incubated for 24 h. Exosomes were prepared from culture supernatants of THP-1 cells by differential centrifugation according to a previously described method.^{44,45}

Exosome Isolation by Commercial Extraction Kits

THP-1 cells were treated with PdNPs (15 μ M), CSP (10 μ M), or GW4869 (20 μ M) and incubated for 24 h, after which the exosomes were isolated and purified using ExoQuick

(EXOQ5TM-1, System Biosciences, Palo Alto, CA, USA) according to the manufacturer's instructions.

Morphological Analysis of Exosomes Using Scanning Electron Microscopy (SEM)

SEM analysis was carried out according to a previously described method.⁴⁶ Pellets containing exosomes were vortexed and resuspended in 0.21 mL of PBS. SEM images were obtained using a field emission scanning electron microscope (HITACHI SU8010, Hitachi Corporation, Japan).

Size and Morphology Analysis of Exosomes Using Transmission Electron Microscopy (TEM)

Sample preparation and analysis were carried out according to a previously described method.⁴⁷ Freshly isolated exosomes from cells were resuspended in cold PBS. Exosome samples were prepared for TEM analysis using the exosome-TEM-easy kit (101Bio, Palo Alto, CA, USA) according to the manufacturer's instructions.

Determination of Total Protein Concentration of Exosomes

Total protein concentration of exosomes was determined using the bicinchoninic acid (BCA) assay kit (Thermo Scientific, Waltham, MA, USA) according to the manufacturer's instructions.

Quantitation of Exosomes Using a Colorimetric Assay

Exosome concentration was estimated using the EXOCETTM assay (System Biosciences), performed as described previously.⁴⁸

Quantification of Exosomes by Fluorescence Polarization (FP)

Quantification of exosomes by fluorescence polarization (FP) was performed as described previously.⁴⁹ Briefly, the exosomes were mixed with 1.6- μ M C12-FAM in a reaction buffer composed of 1-mM HEPES (pH 8) and 1.6-mM NaCl in a total reaction volume of 160 μ L. After the incubation of the reaction mixture for 20 min at room temperature, fluorescence polarization values were

measured at excitation and emission wavelengths of 485 and 528 nm, respectively.

Particle Size and Concentration Analyses

Exosomes were resuspended in PBS, and particle size and concentration were measured using a Nanoparticle Tracking Analysis System 300 (NTA300, Malvern Instruments, UK). Exosome size/diameter was estimated via DLS, as described previously.⁵⁰

Measurement of AChE Activity

AChE activity was determined according to a previously described method.⁵¹ To measure the quantity of exosomes in culture supernatants, cells were treated with PdNPs (15 μ M), CSP (10 μ M), or GW4869 (20 μ M). AChE activity was determined using a commercially available AChE activity assay kit (Sigma).

Sphingomyelinase Activity Assay

THP-1 cells were treated with PdNPs (15 μ M), CSP (10 μ M), or GW4869 (20 μ M) for 24 h. The sphingomyelinase activity assay was performed as previously described⁵² and according to the assay kit manufacturer's protocol. The Amplex Red sphingomyelinase assay kit (Molecular Probes Inc, Eugene, OR, USA) was used to quantify neutral sphingomyelinase activity.

RNA Isolation and mRNA Expression Analysis Using Quantitative Reverse Transcription-Polymerase Chain Reaction (qRT-PCR)

Exosomes were prepared from culture supernatants of THP-1 cells either by differential centrifugation or ExoQuick (EXOQ5TM-1, System Biosciences, Palo Alto, CA, USA) according to a previously described method.⁴⁴ The sequences of the PCR primers are shown in [Supplementary Table 1](#).

Measurements of the Expression Levels of TSG101, CD9, CD63, and CD81 via ELISA

The expression levels of TSG101, CD9, CD63, and CD81 were determined via ELISA, as described previously.⁴⁷

Western Blot

Equal amount of exosomes were mixed with reducing Laemmli-buffer and was loaded on 4–20% Tris-glycine sodium dodecyl sulfate-polyacrylamide gels (Bio-Rad, Hercules, CA, US), and electrophoresed. Proteins were transferred to either polyvinylidene difluoride or nitrocellulose membrane (Bio-Rad, Hercules, CA, US). Membranes were blocked in 5% non-fat milk (Bio-Rad, Hercules, CA, US) in Tris-buffered saline supplemented with 0.05% Tween-20 (TBS-T) for 2h, and then blots were incubated with primary antibodies such as anti-CD63 anti-TSG101 for 16 h at 4°C. After 3 washes in TBS-T, membranes were incubated with corresponding HRP-conjugated secondary antibodies for 2h at room temperature and washed in TBS-T. Signals were visualized after incubation with enhanced chemiluminescence kit.

Measurements of Cytokines and Chemokines

THP-1 cells were incubated with THP-1 cells treated with PdNPs (15 μ M), CSP (10 μ M), or GW4869 (20 μ M) for 24 h. Cytokine and chemokine contents of the exosomes were determined by ELISA.

Statistical Analysis

Independent experiments were repeated at least three times such that data are represented as mean \pm standard deviation (SD) for all duplicates within an individual experiment. Data were analyzed using the *t*-test, multivariate analysis, or one-way analysis of variance (ANOVA), followed by Tukey's test for multiple comparisons to determine the differences between groups (denoted by an asterisk). GraphPad Prism was used for all analyses.

Results and Discussion

Synthesis and Characterization of Palladium Nanoparticles

PdNPs were prepared using nobletin, a citrus flavonoid. Nobletin (5 mg) was suspended in 90 mL of sterile distilled water and mixed for 5 min, followed by the addition of 10 mL of a 1-mM aqueous PdCl₂ solution and incubation for 6 h at 60°C with constant stirring. The color of the reaction mixture changed from yellow to dark brown, indicating the formation of PdNPs.³⁷ This was confirmed using UV-visible spectroscopy ([Figure 1A](#)) by separate comparisons with nobletin solution and PdCl₂. In UV-

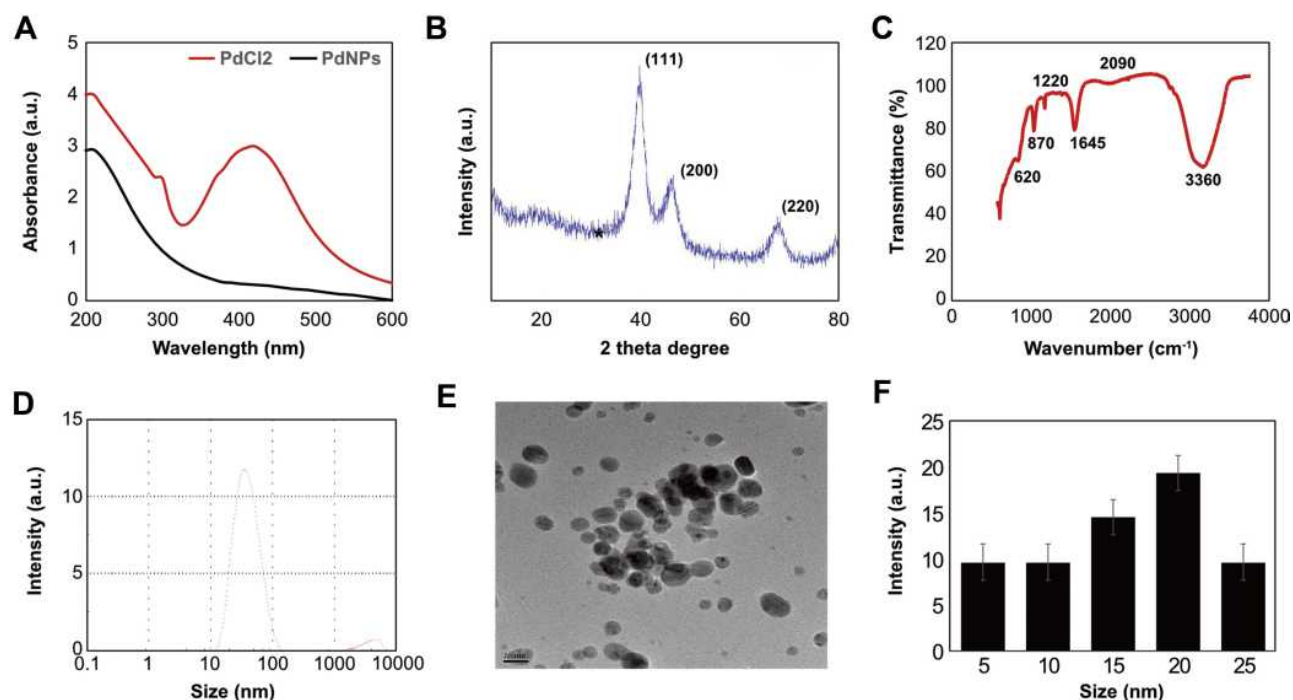


Figure 1 Synthesis and characterization of PdNPs using nobiletin. (A) Absorption spectra of the nobiletin-mediated synthesis of PdNPs; (B) XRD patterns of PdNPs; (C) FTIR spectra of PdNPs; (D) size distribution analysis of PdNPs using DLS; (E) TEM images of PdNPs; and (F) histogram representing the average sizes of particles obtained from TEM images. At least three independent experiments were performed for each sample, and reproducible results were obtained.

visible spectroscopy, the PdCl_2 solution showed a distinct peak at approximately 425 nm, indicating the existence of Pd^{2+} ions. As shown in Figure 1A, at the beginning, a strong characteristic absorption peak at ca. 420 nm was present, corresponding to the $[\text{PdCl}_2]$ ion.⁵³ During the formation of PdNPs, the peak of the Pd^{2+} ions present at 420 nm disappeared and the ion was reduced to Pd^0 . When the reaction proceeded, the peak at 420 nm disappeared almost completely, and the absorption spectrum exhibited a typical light-scattering phenomenon, thus indicating the formation of PdNPs.⁵⁴ During the process, the solution color changed from light yellow to black because of the $[\text{PdCl}_2]$ ion disappearance and formation of PdNPs, indicating that nobiletin potentially reduced PdCl_2 ions to Pd^0 . Silver and PdNPs were synthesized by the coffee and tea extract-mediated green synthesis of silver and PdNPs at room temperature.⁵⁵ Similarly, several studies have reported findings with various biological templates as reducing agents, including *Anacardium occidentale*,⁵⁶ *Pulicaria glutinosa* leaf extract,⁵⁷ *Evolvulus alsinoides* leaf extract,³⁷ *Origanum vulgare* leaf extract.⁵⁸ Other studies have also reported the use of pure biomolecules to facilitate the synthesis of PdNPs such as saponin,⁵⁹ R-phycoerythrin,⁶⁰ hesperidin,⁶¹ and resveratrol.³⁸ Collectively, the data from this study suggest that nobiletin

acts as both a stabilizing and reducing agent, and these biomolecules functionalize the surface of PdNPs.

Next, we analyzed the XRD pattern of PdNPs using nobiletin. As shown in Figure 1B, the XRD patterns of the synthesized PdNPs had prominent peaks. Polyphenol acts as a reducing agent for PdNPs, and the synthesized nanoparticles showed sharp and distinct crystallinity peaks in XRD. A broad peak located at $2\theta = 40.10^\circ$ corresponded to the (111) lattice plane of palladium diffraction pattern. Another two distinct reflections were present in the diffraction at 46.60° (200) and 68.90° (220) (Figure 1B), which represented the face centered cubic (fcc) structure of PdNPs.^{37,38,61} The strong reflection at (111) may specify the desired development track of nanocrystals.^{38,62} Based on the half-width of the (111) reflection, the average crystallite size (~ 25 nm) of PdNPs was calculated using the Debye–Scherer equation. The mean particle size estimated using the Scherrer equation was slightly larger than the real size obtained by TEM.

Further, FTIR analysis was performed to evaluate the interactions of functional groups and nobiletin with palladium (II) ions at room temperature. A typical FTIR spectrum of the PdNPs is shown in Figure 1C. The spectra displayed band at 3360 cm^{-1} could be assigned to the stretching vibration of OH groups related to nobiletin

and 2090 cm^{-1} assigned to the stretching of C=O. However, the bands at 1090 cm^{-1} probably indicated the vibration of C-O-C in nobiletin, and 1645 cm^{-1} indicated the existence of C=C stretching. Moreover, the absorbance bands centered at 1220 , 870 , and 620 cm^{-1} can be assigned to the vibration of $\text{C}=\text{C}$ (aromatic ring). By comparing these results with earlier reports,^{37,38,61} we suggest that the reduction of palladium ions may be performed by the oxidation of hydroxyl groups to carbonyl groups that may participate in the process of nanoparticle synthesis. Similarly, previous studies have reported that using various biomolecules, such as saponin,⁵⁹ R-phycoerythrin,⁶⁰ hesperidin,⁶¹ resveratrol,³⁸ to mediate the synthesis of PdNPs, the mechanism of the reduction of palladium ions may be due to the presence of nobiletin, which play important roles in the redox-type reaction taking place during the reduction of Pd(II) to Pd(0) nanoparticles.^{38,58} Collectively, these findings suggest that the presence of these IR bands in the spectrum of PdNPs suggests that the organic compounds of nobiletin not only act as a bio-reductant but also as capping ligands on the surface of the PdNPs.

Additionally, experiments were performed to determine the size of particles using DLS, which is an effective and essential technique for particle sizing. This technique is also used to measure the hydrodynamic diameter of the particle under the influence of Brownian motion. The average size of the PdNPs was measured by DLS for colloidal nanoparticles. The size distribution vs number percentage graph is shown in Figure 1D. The average size of PdNPs synthesized by nobiletin was 20 nm, and the size varied from 10 to 50 nm. DLS measured the total size of the particles that included the bio-organic compounds enveloping the core of the PdNPs.

Next, we confirmed the size of the synthesized particles by TEM. Figure 1E shows that the TEM images of the as-prepared PdNPs were mostly spherical, with a size range of approximately 5–30 nm and an average size of 20 nm. Figure 1F demonstrates the size distribution from various images of TEM. Several studies have reported similar findings using various biological templates to synthesize various sizes of PdNPs. For example, dried leaf of *Anacardium occidentale* produced PdNPs within the size range of 2.5–4.5 nm,⁵⁶ pine needle extract produced PdNPs with an average size of 11.18 nm,⁶³ R-phycoerythrin synthesized PdNPs with an average size of 25 nm, which were spherical in shape,⁶⁰ *E. alsinoides* synthesized PdNPs within the size range of 1–10 nm, with an average size of 5 nm,³⁷ and *G.*

pedunculata produced PdNPs with an average size of 330 nm,⁶⁴ whereas polypyrrole-palladium nanocomposite particles showed an average diameter of 89 nm in an aqueous dispersion.⁶⁵ PdNPs synthesized using hesperidin, saponin, and resveratrol had average sizes of 10, 5, and 10, respectively.^{37,38,61} The size and shape of nanoparticles mostly depend on various factors, such as the type of reducing agent, concentration of reducing agent, and temperature used for synthesis. Interestingly, the synthesized particles are of small sizes, thus easily and rapidly enter cells or tissues.

Effects of Serum Concentration on Cell Viability, Cell Proliferation, AChE Activity, and Exosomal Protein Concentration of THP-I Cells

Generally, cells are grown in media supplemented with serum. Normally, cell viability and proliferation occur at a slower rate in low serum (1%) than in high serum (10%). To eliminate the high serum effect on exosome production and release, we first evaluated how these cells reacted to the change in culture media to low and high serum concentrations over the course of 24 h. The results demonstrated that the rate of cell viability started to decrease in low serum at 12 h and in high serum at 24 h. These results suggest that regardless of the media, the serum concentration in the media plays a vital role in cell survival. When THP-1 cells were exposed to PdNPs for 24 h, their viability decreased in a time-dependent manner (Figure 2A). Although the cells grown on 10% and 1% sera showed similar trends, the cells grown on RPMI with 10% serum showed 10% viability loss, whereas those grown on RPMI with 1% serum showed 10–30% viability loss at 24 h. Cell viability reduced significantly in a low-serum condition and continuously decreased until 24 h ($p < 0.05$), whereas no significant effect was observed in cells grown in high-serum condition. Similarly, the rate of cell proliferation was significantly affected in cells grown in low-serum medium ($p < 0.05$). The loss of cell proliferation rate was observed at rates of 10 and 30% in 10 serum and 1% serum, respectively (Figure 2B). Particularly, the cell proliferation loss was observed from 10 to 30% ($p < 0.05$). Li et al reported that the proliferation of Neuro2a (N2a, a mouse neuroblastoma cell line) cells grown in a low-serum medium was significantly affected compared to that in a medium containing 10% serum.¹⁹ The cell viability and morphology of human adenocarcinoma cells have also been reported to be significantly affected in a low serum-

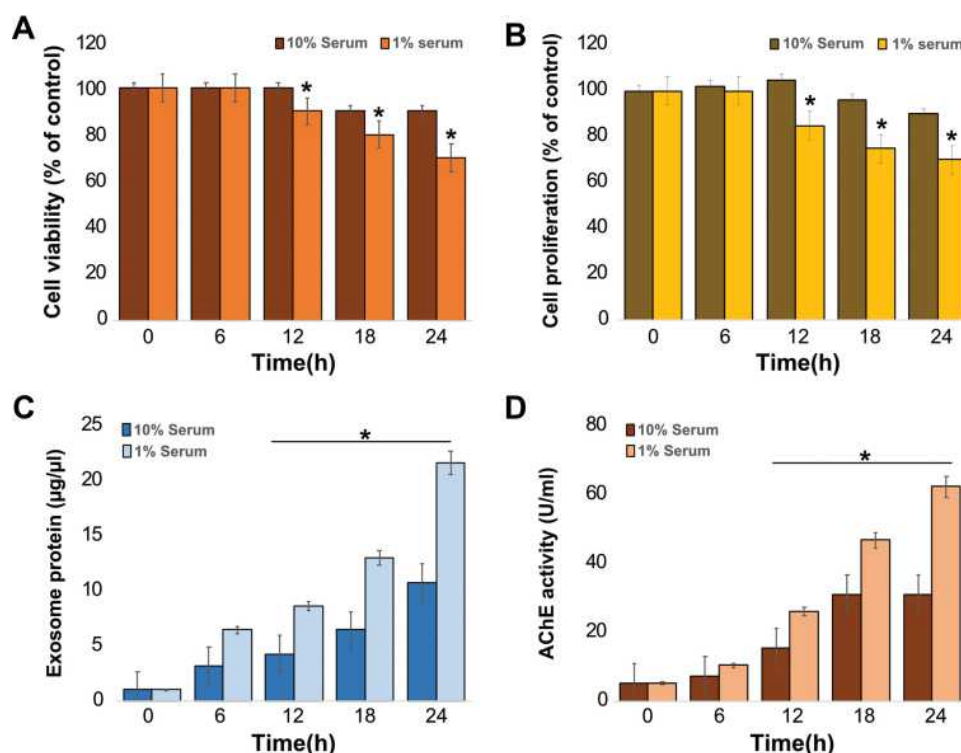


Figure 2 Effects of serum on cell viability, proliferation, exosome protein, and AChE activity on THP-1 cells. THP-1 cells were grown in RPMI-1640 cell culture medium supplemented with 10% fetal calf serum (FCS) or 1% FCS over a 24 h period. **(A)** Cell viability was determined using the CCK-8 assay. **(B)** Cell proliferation was determined using BrdU. **(C)** Total protein concentration of isolated exosomes was determined using BCA. **(D)** AChE activity was determined from isolated exosomes using a colorimetric method. The results are expressed as the mean \pm standard deviation of three independent experiments. The treated groups showed statistically significant differences from the control group by the Student's *t*-test; **p* < 0.05 was considered significant.

containing medium, and the cellular protein levels of chloride intracellular channel protein 1, proteasome subunit alpha type 2, and heat shock 70 kDa protein 5 were dysregulated in A549.⁶⁶ Collectively, the data from these studies suggest that serum has a significant effect on cell viability and proliferation of THP-1 cells.

Next, to determine the correlation between AChE activity and serum concentration in the media, THP-1 cells were grown in both media containing 1 and 10% sera for 24 h, followed by exosome isolation and protein quantification. As expected, a low serum concentration produced a significantly higher amount of exosomal protein compared to that produced by a high concentration of serum, and the exosomal protein concentration was time dependent (Figure 2C). Similarly, Li et al found that amounts of exosomes were significantly higher in cells grown on low-serum media than in cells grown on high-serum media.¹⁹ Additionally, Rashid and Coombs have previously evaluated the effect of serum on the expression of HSP45 in A549 cells.⁶⁶ Consistent with these results, we found that the total protein concentration of exosomes was higher in low serum-containing media than in media

containing high serum, suggesting that low serum concentration in a medium is suitable for producing a high amount of exosomes in THP-1 cells.

Further, we investigated the correlation between protein concentration of exosomes and AChE activity of exosomes in THP-1 cells. The cells were grown in both 10 and 1% serum concentrations, and AChE activity was determined. AChE activity indirectly determines the quantity of exosomes because AChEs are localized to the membrane of exosomes.^{51,67} Our results demonstrated that the activity of AChE is dependent on time and serum concentration, showing that media containing 1% serum exhibited high levels of AChE activity compared to media containing 10% serum (Figure 2D). AChE activity was significantly higher in lipopolysaccharide (LPS)-treated macrophages than in untreated groups.⁵¹ The correlation between cell proliferation and AChE activity has been previously demonstrated via the inhibition of AChE activity, leading to an increase in cell proliferation, which was associated with the downregulation of p27 and cyclins in hepatocellular carcinoma cells.⁶⁸ Collectively, these findings indicate that decreased cell proliferation owing to low serum concentration increases

exosome biogenesis and AChE activity. Further we determined the concentration of exosomes isolated by ultracentrifugation (Supplementary Figure 1A) and ExoQuick (Supplementary Figure 1B) from THP-1 cells using standard ExoQuick reagents. The results depicted that the concentration of exosomes were isolated from ultracentrifugation remarkably lower compared to exosomes were isolated from ExoQuick. Therefore, further experiments were carried out exosomes were isolated from ExoQuick.

Dose-Dependent Effects of PdNPs, CSP, and GW4869 on THP-1 Cells

To determine the cytotoxic effects of PdNPs, CSP, and GW4869 on THP-1 cells, the cells were treated with various PdNP concentrations (5–25 μ M), CSP (5–25 μ M), and GW4869 (5–25 μ M) for 24 h, and cell viability was determined using CCK-8 assay kit. PdNPs showed a concentration-dependent effect in THP-1 cells. The cell viability of THP-1 cells decreased significantly upon exposure to PdNPs at concentrations ranging from 5 to 25 μ M, and IC₅₀ was found to be 15 μ M (Figure 3A). Similarly, while cells were exposed to CSP, cell viability declined dose dependently, which was used as a positive control, and IC₅₀ was found to be 10 μ M

(Figure 3B). Both PdNPs and CSP showed similar trends, and the relative loss of cell viability appeared to be similar. PdNPs potentially induce cell viability loss in a variety of cell lines with different nanostructures. Cell viability reduction was observed when HeLa cells were exposed to Pd–Au heterostructures irradiated with 808 nm laser light.⁶⁹ PdNPs induce loss of cell viability in human ovarian cancer cells via oxidative stress.³⁷ Palladium(II) complexes such as [Pd(sac)(terpy)](sac)·4H₂O and [PdCl(terpy)](sac)·2H₂O reportedly showed dose-dependent cytotoxic effects against three human leukemia cell lines including Jurkat, MOLT-4, and THP-1.⁷⁰ Biologically synthesized PdNPs have also shown significant cytotoxicity in human cervical cancer cells,⁵⁹ peripheral lymphocytes non-cancer cells,⁷¹ and human lung carcinoma cells.³⁸ In contrast, the cells treated with GW4869 (5–25 μ M), which were used as negative controls, exhibited no toxic effect, and no significant reduction was observed in cell viability (Figure 3C). Similarly, RAW264.7 macrophages exposed to GW4869 up to 20 μ M showed no toxic effect.

Next, we determined the dose-dependent effect of PdNPs (5–25 μ M), CSP (5–25 μ M), and GW4869 (5–25 μ M) on THP-1 cell proliferation. Although both cell viability and proliferation are similar in that both are

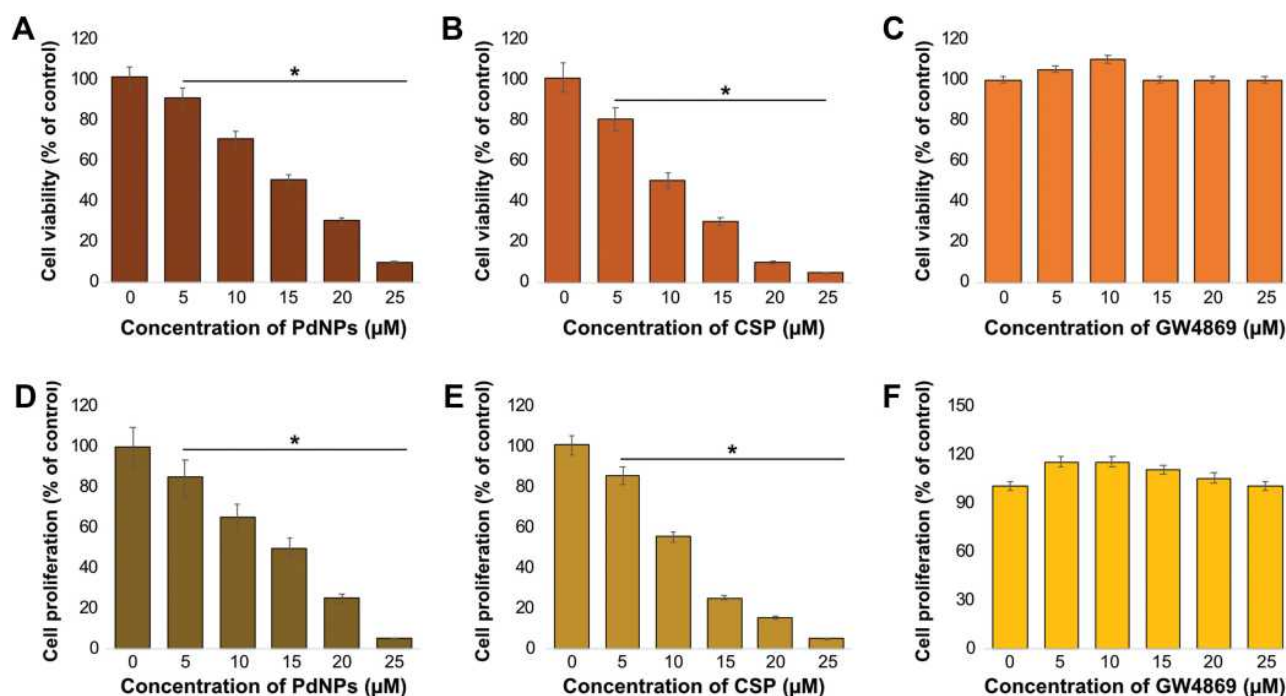


Figure 3 Dose-dependent effects of PdNPs, CSP, and GW4869 on the viability and proliferation of THP-1 cells. THP-1 cells were treated with various concentrations of (A) PdNPs (5–25 μ M), (B) CSP (5–25 μ M), and (C) GW4869 (5–25 μ M) in RPMI-1640 cell culture medium supplemented with 1% FCS for 24 h, and cell viability was determined using CCK-8. Cell proliferation was determined by BrdU in THP-1 cells exposed to (D) PdNPs (5–25 μ M), (E) CSP (5–25 μ M), and (F) GW4869 (5–25 μ M). The results are expressed as the mean \pm standard deviation of three independent experiments. The treated groups showed statistically significant differences from the control group by the Student's *t*-test; **p* < 0.05 was considered significant.

measures of live cells, viability is a measure of cellular activity and overall health, while proliferation is a measure of the rate of growth and production of daughter cells of a cell population. THP-1 cells were treated with various PdNP concentrations (5–25 μ M), CSP (5–25 μ M), and GW4869 (5–25 μ M) for 24 h, and cell proliferation level was determined using a BrdU assay kit. PdNPs showed a concentration-dependent effect in THP-1 cells, with a significant decrease in THP-1 cell proliferation upon exposure to PdNPs at concentrations ranging from 5 to 25 μ M (Figure 3D). Similarly, cell proliferation declined following exposure to CSP (Figure 3E). Gurunathan et al reported that biomolecule-assisted PdNPs potentially reduce the rate of cell proliferation in human ovarian and human lung cancer cells.^{37,38} Additionally, PdNPs have been reported to inhibit cell growth in a dose- and time-dependent manner in fibroblasts and lung epithelial cells.⁷² In contrast, when cells were exposed to GW4869, no significant effect on cell proliferation rate was observed (Figure 3F). Our results are in significant agreement with those of Cheng et al, who reported that cell proliferation rate decreased when the concentration of GW4869 was ≥ 40 μ mol/L.⁴⁴ Collectively, both PdNPs and CSP dose-

dependently decreased the viability and proliferation of THP-1 cells, whereas GW4869 had no effect on these activities. Therefore, all our experiments were carried out with specific concentrations of PdNPs (15 μ M) and CSP (10 μ M) because they produced the optimal effect of approximately $50 \pm 5\%$ survival after 24 h treatment. In the case of GW4869, we used 20 μ M because it is non-toxic.

Effect of PdNPs on THP-1 Cell Cytotoxicity

To evaluate the cytotoxic effect of PdNPs on THP-1 cells, we performed various types of assays such as cell viability, cell proliferation, cell death, and leakage of LDH. The cells were treated with PdNPs (15 μ M), CSP (10 μ M), or GW4869 (20 μ M) for 24h. To know the potency of PdNPs, we performed a CCK-8 assay. Cells were grown in low-serum medium in the presence of PdNPs. Media supplemented with PdNPs have been shown to reduce cell viability. After 24 h of PdNPs and CSP treatments, THP-1 cells showed significant loss in viability up to 50 and 55%, respectively. In contrast, GW4869-treated THP-1 cells showed no significant difference in viability (Figure 4A).

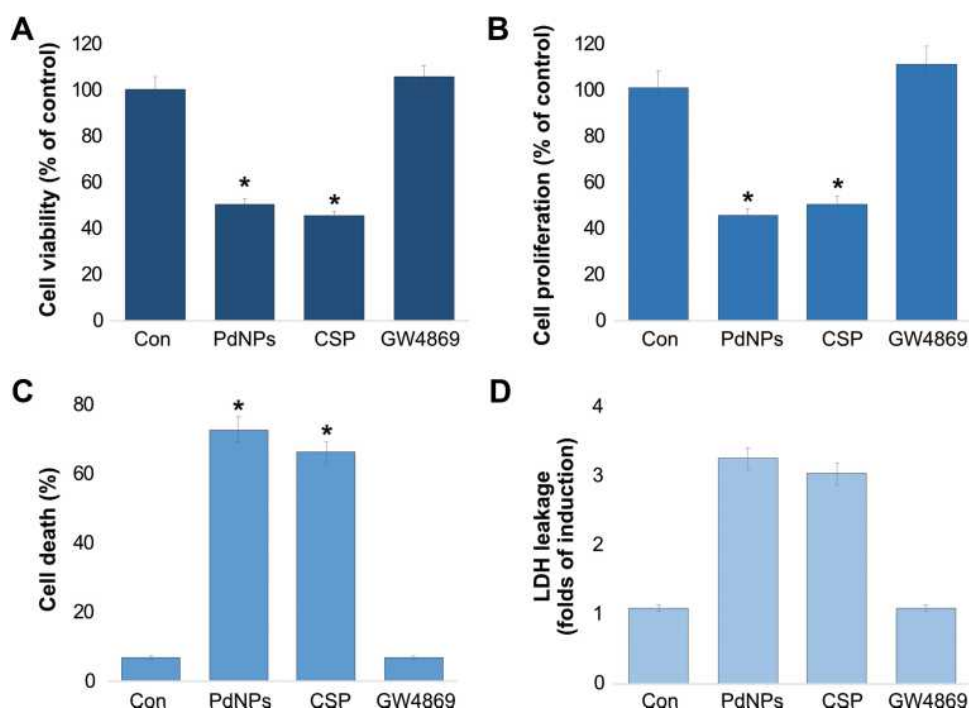


Figure 4 Effect of PdNPs on the cytotoxicity of THP-1 cells. THP-1 cells were treated with PdNPs (15 μ M), CSP (10 μ M), or GW4869 (20 μ M) in RPMI-1640 cell culture medium supplemented with 1% FCS for 24 h. (A) Cell viability was determined using the CCK-8 assay (B). Cell proliferation was determined by BrdU, (C) cell death rate was determined using trypan blue, and (D) LDH leakage was measured at 490 nm using the LDH cytotoxicity kit. The results are expressed as the mean \pm standard deviation of three independent experiments. The treated groups showed statistically significant differences from the control group by the Student's *t*-test; **p* < 0.05 was considered significant.

These results clearly demonstrate that PdNPs and CSP have toxic effects and support the results of cell proliferation (Figure 4B). To substantiate the data derived from cell viability and proliferation, trypan blue experiments were carried out to determine cell death and membrane integrity of the samples. Our findings further confirmed that PdNPs and CSP induced 55 and 50%, respectively (Figure 4C). This is consistent with cell viability and proliferation data, showing a strong direct correlation. The cytotoxic effects of PdNPs and CSP were evaluated by analyzing LDH release from THP-1 cells for 24 h, as shown in Figure 4D. LDH release was expressed as a fold increase relative to LDH release from untreated cells. Our results showed that treatment of THP-1 cells with PdNPs and CSP induced a significant release of LDH from THP-1 cells with 3.0 and 2.8 folds, respectively, indicating the disruption of the cell membrane structure. The efficacy of PdNPs depends on their size, shape, physical and chemical properties, and cell type.^{59,73} For instance, PdNPs with an average size of 5 nm potentially induce cytotoxicity by inducing loss of cell viability, proliferation, and increasing cell death rate and leakage of LDH. Similarly, several studies have reported the cytotoxic effect of PdNPs in

various types of cancer cells, including human ovarian cancer cells.^{37,61} Further PdNPs potentiate cytotoxicity with histone deacetylase (HDAC) inhibitors. For example, the combination of PdNPs with tuastatin or trichostatin A has been reported to significantly induce cytotoxicity and apoptosis in various types of cancer cells, including human ovarian cancer cells, human breast cancer cells, and human lung epithelial adenocarcinoma cells.^{38,59,60}

PdNPs Induce Oxidative Stress Markers in THP-1 Cells

Generally, when nanoparticles enter cells, they produce adverse effects. The most validated explanation for the cytotoxicity of nanoparticles is that oxidative stress is induced by an ROS burst, which causes damage to cellular structures and alters the normal physiological functions of cells by attacking various biomolecules, including carbohydrates, nucleic acids, unsaturated fatty acids, and proteins.⁷⁴ To determine the influence of PdNPs on oxidative stress in THP-1 cells, the cells were incubated with PdNPs (15 μ M), CSP (10 μ M), or GW4869 (20 μ M) for 24 h, and the level of ROS was measured. As expected, treatment of THP-1 cells with either PdNPs or CSP increased the production of ROS (Figure 5A),

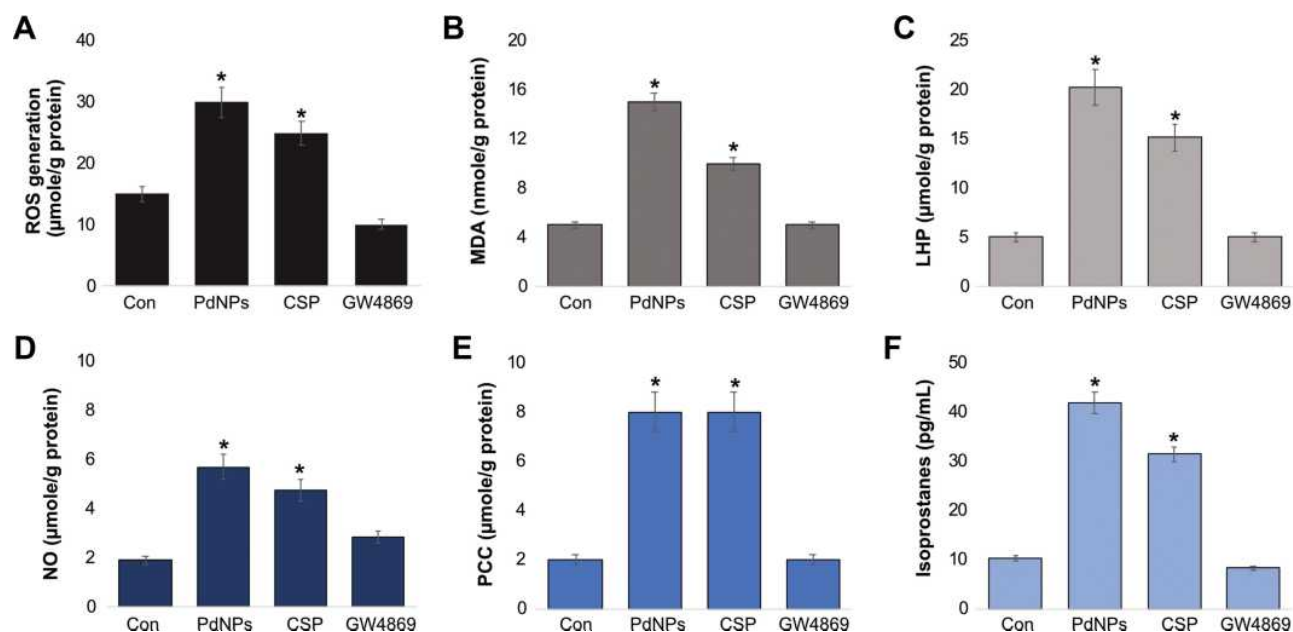


Figure 5 Effect of PdNPs on oxidative stress markers. THP-1 cells were treated with PdNPs (15 μ M), CSP (10 μ M), or GW4869 (20 μ M) in RPMI-1640 cell culture medium supplemented with 1% FCS for 24 h. (A) Spectrophotometric analysis of ROS was performed using 2',7'-dichlorodihydrofluorescein diacetate (DCFH-DA). (B) Malondialdehyde concentration was measured using a thiobarbituric-acid-reactive substances assay and expressed as nanomoles per gram of protein. (C) Lipid hydroperoxides were extracted and quantified as indicated using the Lipid Hydroperoxide Assay Kit (Catalog No. 705003; Cayman Chemical Company). (D) Nitric oxide production was quantified spectrophotometrically using Griess reagent and expressed as micromoles per gram of protein. (E) Protein carbonylation content was determined and expressed as micromoles per gram of protein. (F) 8-Isoprostane was quantified using the protocol described in the ELISA Kit (Catalog No. 516351, Cayman Chemical Company) manual. The results are expressed as the mean \pm standard deviation of three independent experiments. The treated groups showed statistically significant differences from the control group by the Student's *t*-test; **p* < 0.05 was considered significant.

whereas GW4869-treated cells exhibited no change compared to untreated cells. THP-1 cells treated with PdNPs, CSP, and GW4869 produced 30, 25, and 10 μmol of ROS, respectively, compared to that by untreated cells (15 μmol). Both PdNPs and CSP significantly induce ROS generation. Similarly, metal nanoparticles such as silver induce oxidative stress in male somatic and spermatogonial stem cells,⁷⁵ F9 teratocarcinoma stem cells,⁷⁶ mouse embryonic fibroblast cells,⁷⁷ and various types of human cancer cells including human breast^{78,79} and human lung cancer cells^{80,81} via the generation of ROS. Similarly, platinum nanoparticles cause oxidative stress in THP-1 cells,⁸² and PdNPs induce oxidative stress and eventual cell death in human ovarian cancer cell lines A2780³⁷ and SKOV3.⁶¹

Next, we examined another oxidative stress marker called malondialdehyde (MDA), which is a biomarker of widely studied products of lipid peroxidation. Lipid peroxidation plays a significant role as an important secondary messenger in the process of adaptation/commitment to apoptosis.⁸³ Lipid peroxidation products regulate pathways responsible for the antioxidant protection system. The most commonly studied secondary products of lipid peroxidation include MDA, propanal, hexanal, and 4-hydroxynonenal (4-HNE). THP-1 cells were incubated with PdNPs (15 μM), CSP (10 μM), or GW4869 (20 μM) for 24 h, and MDA level was measured. The levels of MDA were 15, 10, and 5 μmol , respectively (Figure 5B). Because of ROS generation, cell destruction could be observed by the final product of lipid peroxidation, such as MDA. Increased levels of MDA are one of the main results of lipid peroxidation. It has been reported that the oxidative effect of metal nanoparticles is much more than that of non-metal nanoparticles.³⁸ Further, we have shown that various metal nanoparticles stimulate toxicity, oxidative stress, and DNA damage in various types of cancer cells, which may be partly due to the dissolved ionic nature of metal nanoparticles. For example, PdNPs can induce significant levels of MDA in human ovarian cancer cells.⁶¹ The combination of PdNPs with tuastatin or trichostatin A has also significantly induced MDA in various types of cancer cells including human ovarian cancer cells, human breast cancer cells, and human lung epithelial adenocarcinoma cells.^{38,59,60}

Measurement of lipid hydroperoxides (LHP) is a valuable method that is widely used to evaluate oxidative catabolism of lipid membranes. To further prove the effect of PdNPs on the oxidative catabolism of polyunsaturated fatty acids, we measured the level of LHP. Oxidative stress is the principal factor of lipid peroxidation, which

prompted us to measure the LHP after 24 h exposure to PdNPs. Hence, we measured the level of LHP after 24 h incubation with PdNPs (15 μM), CSP (10 μM), or GW4869 (20 μM). An increased amount of LHP was observed in cells grown under conditions of PdNPs and CSP, exhibiting 20 and 15 μmol , respectively, whereas GW4869-treated cells showed no remarkable changes compared to controls (Figure 5C). AgNPs activate the processes of lipid peroxidation and, owing to increases in the levels of lipid peroxidation, lead to morphological changes in human lymphocytes.⁸⁴ Moreover, results from the present study are in significant agreement with those of previous studies suggesting that the toxicity of PdNPs is mediated by ROS and oxidative stress. PdNPs or a combination of PdNPs and melatonin reportedly increased the levels of LPH in human lung epithelial adenocarcinoma cell lines A549 and H1229.³⁸ Paciorek et al⁸⁵ have also reported that silver nanoparticles increase the level of lipid peroxides in AgNP-treated Hep G2 cells.

Further, we assessed the levels of NO in THP-1 cells exposed to PdNPs (15 μM), CSP (10 μM), or GW4869 (20 μM) for 24 h. Our results showed that both PdNPs and CSP increased NO level. The level of NO was 6 and 5 μmol , respectively, whereas the level of NO in GW4869-treated cells was 3 μmol compared to that in the control (2 μmol) (Figure 5D). Effective anticancer activity and oxidative stress have been associated with increasing NO levels, which were observed in various types of cancer cells, including pancreatic, colon, and ovarian cancer cells.⁸⁶ Increased levels of NO upregulate nitro-oxidative stress and cell death mediators.⁸⁷ Our previous study demonstrated an increase in NO level in F9 teratocarcinoma stem cells following retinoic acid treatment.⁸⁸ Additionally, platinum nanoparticles have been shown to increase the levels of NO in THP-1⁴⁰ and human neuroblastoma cells,⁸⁹ and PdNPs and a combination of PdNPs and melatonin reportedly increased NO level in human lung epithelial adenocarcinoma cells.³⁸ The increased level of NO could be a causative factor for cell death and the pro-inflammatory effect of PdNPs.

Further, measurement of protein carbonylation content (PCC) is a multipurpose and sensitive method to describe NP-induced oxidative stress. Therefore, we measured the level of PCC in THP-1 cells exposed to PdNPs (15 μM), CSP (10 μM), or GW4869 (20 μM) for 24 h. PCC levels in PdNPs- and CSP-treated cells were 8 and 8 μmol , respectively, whereas the level of PCC was 2 μM in GW4869-treated THP-1 cells, which was equivalent to that in the control group (Figure 5E). Several studies have reported

that metal nanoparticles such as AgNPs induce PCC in THP-1 macrophages, primary neuronal cells,⁹⁰ and a human colon epithelial cell line.⁹¹ Our previous studies also demonstrated that platinum nanoparticles, doxorubicin, cisplatin, and a combination of platinum nanoparticles and doxorubicin induced PCC in human bone OS epithelial cells (U2OS),⁹² and platinum nanoparticles increased the level of PCC in THP-1 cells.⁴⁰ Combination of PdNPs and melatonin elevates PCC level in human lung epithelial adenocarcinoma cells.³⁸ The amount of PCC is directly correlated with the severity of oxidative stress, and elevated PCC level in THP-1 macrophages exerts strong cytotoxicity and oxidative stress.

Oxidative stress is caused by nanoparticle-induced toxicity in cells and eventually leads to cell death. To evaluate the role of PdNP-induced oxidative stress in THP-1 cells, we measured 8-Isoprostane, which is a dependable biomarker of oxidative stress, as it is produced by the oxidation of phospholipids. To measure the level of 8-isoprostane, THP-1 cells were treated with PdNPs (15 μ M), CSP (10 μ M), or GW4869 (20 μ M) for 24 h. Results indicate that 8-isoprostane levels were significantly increased in treated cells compared to those in untreated cells (Figure 5F). The levels of 8-Isoprostane in PdNP-, CSP-, and GW4869-treated cells were 40, 30, and 8 μ mol, respectively. Both PdNPs and CSP

significantly increased 8-Isoprostane level, whereas GW4869 had no effect on the amount of 8-Isoprostane. A previous study reported that HEp-2 cells exposed to copper oxide nanoparticles induced a significant increase in the level of 8-isoprostanes.⁹³ Additionally, rats exposed to nano-aerosol showed a 1.8-fold increase in LDH activity and 8-isoprostane concentration in BALF.⁹⁴ Combination of PdNPs and melatonin also increased the level of 8-isoprostane in human lung epithelial adenocarcinoma cells.³⁸ Collectively, our findings suggest that PdNPs potentially induce cytotoxicity, oxidative stress, nitro-oxidative stress, lipid peroxidation, and protein carbonylation. These stress factors could eventually cause an imbalance in pro and antioxidant levels.

Influence of PdNPs on Antioxidants Markers in THP-1 Cells

Since antioxidants balances free radical or reactive oxygen species production, we measured various antioxidant systems in THP-1 cells treated with PdNPs (15 μ M), CSP (10 μ M), or GW4869 (20 μ M) for 24 h, such as glutathione (GSH), thioredoxin (TRX), catalase (CAT), superoxide dismutase (SOD), glutathione peroxidase (GPx), and glutathione S-transferases (GST), which are indispensable molecules for anti-oxidative defense. GSH is an important intracellular molecule responsible for maintaining the pro

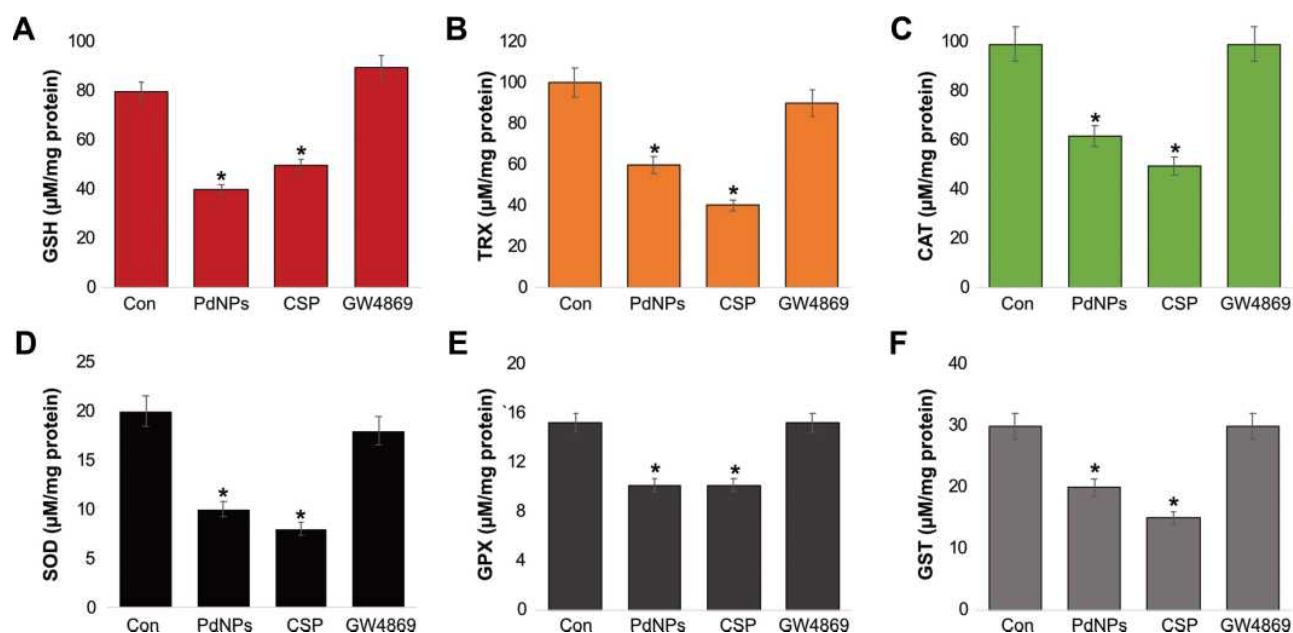


Figure 6 Effect of PdNPs on antioxidants. THP-1 cells were treated with PdNPs (15 μ M), CSP (10 μ M), or GW4869 (20 μ M) in RPMI-1640 cell culture medium supplemented with 1% FCS for 24 h. (A) GSH, (B) TRX, (C) CAT, (D) SOD, (E) GPX, and (F) GST concentrations are expressed as micromoles per milligram of protein. The results are expressed as the mean \pm standard deviation of three independent experiments. The treated groups showed statistically significant differences from the control group by the Student's *t*-test; **p* < 0.05 was considered significant.

and antioxidant buffer system and is the most abundant cellular thiol compound.⁹⁵ Our results demonstrated that PdNPs and CSP significantly decreased the level of GSH, with levels 40 and 50 μmol , respectively, compared to that in the control group (80 μmol). GW4869-treated cells showed slightly increased levels of GSH (90 μmol) when compared to that in the control (Figure 6A). Similarly, previous studies have reported decreases in GSH levels in different types of cancer cells. For instance, graphene oxide decreases the level of GSH in human embryonic kidney cells,⁹⁶ and THP-1 cells,⁹⁷ and platinum and PdNPs increase GSH levels in THP-1 and human lung epithelial adenocarcinoma cells, respectively.^{38,40}

Next, we measured the level of TRX in THP-1 cells exposed to PdNPs (15 μM), CSP (10 μM), or GW4869 (20 μM) for 24 h. Results showed that PdNPs and CSP significantly decreased the level of TRX, with levels 60 and 40 μmol , respectively, compared to that in the control group (100 μmol). GW4869-treated cells showed slightly increased levels of TRX (90 μmol) when compared to that in the control (Figure 6B). TRXs are ubiquitous antioxidant enzymes that play significant roles in maintaining cellular redox balance in cancer cells. F9 teratocarcinoma stem cells exposed to retinoic acid showed a decrease the level of TRX.⁸⁸ Ultra-small- and medium-sized platinum nanoparticles decreased the levels of TRX in THP-1 cells.^{40,82} TRX and GSH are major thiol-dependent antioxidants involved in maintaining cell homeostasis and DNA synthesis and repair.⁹⁸

Further, we analyzed the status of CAT and SOD, which are significant antioxidants for maintaining the level of ROS in organisms and are used as bio-indicators of increased ROS production.⁹⁹ To determine the levels of CAT and SOD, THP-1 cells were treated with PdNPs (15 μM), CSP (10 μM), or GW4869 (20 μM) for 24 h. The concentration of CAT was 50 and 40 μmol in PdNP- and CSP-treated cells, respectively, whereas cells treated with GW4869 showed 80 μM CAT concentration, which was equivalent to that of the control, indicating that GW4869 has no effect on CAT activity (Figure 6C). In contrast, PdNPs and CSP significantly influenced CAT activity. We have previously shown that different shapes and sizes of platinum nanoparticles decrease CAT activity in THP-1 cells.^{40,82} Similarly, the level of SOD was significantly lower in cells treated with PdNPs (10 μmol) and CSP (8 μmol) than in control cells, whereas GW4869-treated cells showed no significant effect (18 μmol) on CAT activity compared to the control (20 μmol) (Figure 6D). The concentrations of CAT and SOD were reportedly significantly compromised in PdNP-exposed human ovarian cancer cells,³⁷

human cervical cancer cells,⁵⁹ human breast cancer cells,⁶⁰ and human lung epithelial adenocarcinoma cells.³⁸ Combination of graphene oxide-silver nanoparticle nanocomposites and CSP decreases the level of SOD in human cervical cancer cells.¹⁰⁰ Nanoparticles can interfere with the expression of antioxidant genes, such as SOD and GPX, and instability in the expression of antioxidant genes leads to the accumulation of ROS.

Further, we examined the levels of GPX and GST in THP-1 cells exposed to PdNPs (15 μM), CSP (10 μM), or GW4869 (20 μM) for 24 h and found that both PdNPs and CSP decreased the intracellular concentration of GPX and GST. The concentrations of GPX in PdNP- and CSP-treated cells were 10 and 10 μmol , respectively, whereas GPX concentration in GW4869-treated cells was equal to that in the control (15 μmol) (Figure 6E). The concentrations of GST in PdNP- and CSP-treated cells were 20 and 15 μmol , respectively, whereas the cells treated with GW4869 had equal GST concentration to that of the control (30 μmol) (Figure 6F). Niska et al previously reported that exposure of mouse hippocampal HT22 cells to CuO nanoparticles decreased the levels of antioxidant molecules such as GSH and detoxification enzymes such as GPx, SOD, and GST, as well as the gene expression levels of GPx and SOD in the cells.¹⁰¹ Collectively, the possible reason for the decreased levels of all tested antioxidant markers including GSH, TRX, CAT, SOD, GPx, and GST is the increased oxidation of thiol groups to overcome the increased level of ROS in cells incubated with either PdNPs or CSP. Administration of AgNPs into rats has been shown to decrease the levels of GSH, GST, and CAT.¹⁰² Moreover, the concentrations of GPX and GST were significantly decreased in PdNP-exposed human ovarian cancer cells,³⁷ human cervical cancer cells,⁵⁹ human breast cancer cells,⁶⁰ and human lung epithelial adenocarcinoma cells,³⁸ while the combination of PdNPs and tubastatin A decreased GST level in human breast cancer cells.⁶⁰ Altogether, due to the strong oxidation potential of PdNPs, excessive levels of pro-oxidants and low levels of antioxidants lead to oxidative stress, protein oxidative carbonylation, lipid peroxidation, DNA/RNA breakage, and membrane structure destruction, eventually causing cell death.

PdNPs Induce ER Stress in THP-1 Cells

Environmental or nanoparticle-induced stress on cells causes disturbances to various organelles, including the endoplasmic reticulum (ER). ER stress ultimately induces apoptosis and is involved in various pathological conditions. Because of ER stress, a loss of homeostasis occurs in the ER and leads to accumulation of misfolded proteins in the ER lumen. ER

stress activates a series of adaptive mechanisms known as the unfolded protein response¹⁰³ and has been reported to promote the release of extracellular vesicles (EVs) carrying pro-inflammatory damage-associated molecular pattern molecules in BeWo choriocarcinoma cells.¹⁰⁴ Hence, we investigated the effect of PdNPs and CSP on ER stress and the induction of the UPR. Six well-known ER stress markers including IRE, PERK, ATF-6, ATF-4, GRP78, and CHOP were assessed. THP-1 cells were exposed to PdNPs (15 μ M), CSP (10 μ M), or GW4869 (20 μ M) for 24 h, followed by quantification of IRE, PERK, ATF-6, ATF-4, GRP78, and CHOP mRNAs. PdNPs led to a strong induction of all tested genes (from 2 to 5 fold) in treated cells compared to those in the control. Similarly, CSP strongly induced all tested genes (from 2 to 4 fold), while GW4869-treated cells exhibited no induction of these genes (Figure 7A–F). Among all the genes, PERK showed the strongest expression, and CHOP showed a moderate expression. These data suggest that exposure to PdNPs leads to ER stress and the associated induction of UPR. CSP induces various ER stress-related genes in SH-SY5Y cells.⁸⁹ Several studies have reported that various metal nanoparticles such as ZnONPs increase the phosphorylation of RNA-dependent PERK, and eukaryotic initiation factor 2 decreased protein translation and synthesis.¹⁰⁵ The activation of IRE, PERK, ATF-6, ATF-4, GRP78, and CHOP in THP-1 cells by PdNPs was consistent with the results of

previous studies performed using various nanoparticles, such as those of titanium dioxide¹⁰⁶ and zinc oxide.¹⁰⁵ We have previously shown that platinum nanoparticles induce the expression of ER stress-related genes in THP-1 cells.⁸² Additionally, the combination of platinum nanoparticles and retinoic acid induces the expression of ER stress-related genes in human neuroblastoma cells.⁸⁹ Two different sizes of silver nanoparticles reportedly induced ER stress breast cancer cells by the accumulation and aggregation of misfolded proteins and activation of the unfolded protein response UPR. AgNPs have also been shown to activate the three main ER sensors, PERK, IRE-1 α and ATF-6,¹⁰⁷ and silica.^{108,109} Severe ER stress resulting in CHOP upregulation and cell death resulted in the production of EVs carrying pro-inflammatory damage-associated molecular pattern.¹⁰⁴ These findings clearly suggest that PdNP-induced ER stress is possible for apoptosis.

PdNPs Induce Mitochondrial Dysfunction, Caspase Activation, and DNA Damage

Although ROS play important roles in physiological processes, excessive ROS cause redox imbalance, which can lead to apoptosis. Oxidative stress and mitochondrial damage are interrelated physiological processes in various diseases. Oxidative stress and ER are known to induce damage to the mitochondrial respiratory chain, alter

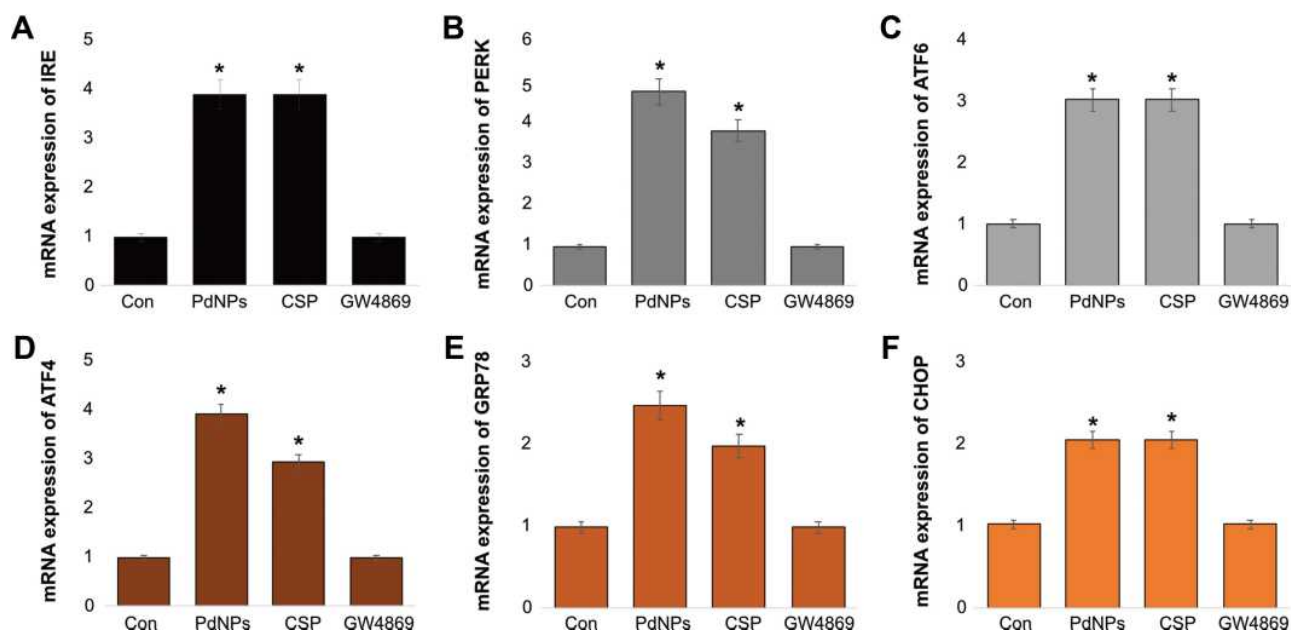


Figure 7 Effect of PdNPs on ER stress. THP-1 cells were treated with PdNPs (15 μ M), CSP (10 μ M), or GW4869 (20 μ M) in RPMI-1640 cell culture medium supplemented with 1% FCS for 24 h. The mRNA expression of ER stress markers including IRE, PERK, ATF-6, ATF-4, GRP78, and CHOP (A–F) were estimated via qRT-PCR. The results are expressed as the mean \pm standard deviation of three independent experiments. The treated groups showed statistically significant differences from the control group by the Student's *t*-test; **p* < 0.05 was considered significant.

membrane permeability, and influence Ca^{2+} homeostasis and mitochondrial defense systems. Therefore, to determine the effect of PdNPs on mitochondrial dysfunction, THP-1 cells were treated with PdNPs (15 μM), CSP (10 μM), or GW4869 (20 μM) for 24 h, and the loss of mitochondrial membrane potential was assessed by the JC-1 assay. The cells treated with PdNPs and CSP showed significant reduction in MMP activity up to 30 and 40%, respectively, compared to the control. In contrast, cells treated with GW4869 had no effect on MMP activity (Figure 8A). Several studies have shown that metal nanoparticles induce loss of membrane potential in several types of cancer cells, including human cervical cancer cells,⁵⁹ human breast cancer cells,⁶⁰ human alveolar basal epithelial cells,¹¹⁰ human ovarian cancer cells,¹¹¹ human osteosarcoma cells,⁹² human lung epithelial adenocarcinoma cells A549 and H1229,³⁸ and human neuroblastoma cells.⁸⁹ Collectively, PdNPs induce mitochondrial dysfunction.

Apoptotic pathways are mainly regulated by caspases. Major caspases consist of upstream initiators such as caspases-8, -10, -2, and -9 and downstream effectors such as caspases-3, -6, and -7. To determine the activation of caspases by PdNPs, we selected caspase-9 and -3 and measured the levels of caspases in THP-1 cells exposed to PdNPs (15 μM), CSP (10 μM), or GW4869 (20 μM) for 24 h. The cells treated with PdNPs and CSP showed

significant activation of caspase-9 up to 3.5 and 3.0 folds and caspase-3 up to 4.0 and 3.0 folds, respectively, compared to those in the control. Conversely, cells treated with GW4869 had no effect on both caspase-9 and caspase-3 (Figure 8B and C). Several studies have provided support for the activation of caspases by various metal nanoparticles. PdNPs induce caspase-3 activation in human ovarian cancer cells,³⁷ and AgNPs have shown dose-dependent cytotoxicity through the activation of the caspase 3 in DLA cells,¹¹² human breast cancer cells,³⁹ and human ovarian cancer cells.¹¹³ Combination of PdNPs with trichostatin A or tubastatin A can activate caspase-3 activation in human breast cancer cells,^{59,60} while platinum nanoparticles reportedly induce caspase 3 in various types of cancer cells, including prostate,¹¹⁴ human neuroblastoma cancer cells,⁸⁹ and THP-1 cells.⁸²

Further, 4-hydroxynonenal (4-HNE) is a destructive oxidized by-product of lipid peroxidation, and the level of 4-HNE determines the level of oxidative stress in a cell. The concentration of 4-HNE is produced within the range of 0.1–3 μM under physiological conditions and under oxidative stress conditions. The concentration of 4-HNE that accumulates in membranes ranges from 10 μM to 5 mM.¹¹⁵ Protein dysfunction can be induced by 4-HNE, which induces cellular apoptosis and death. To determine whether PdNPs induce elevated 4-HNE levels, we first measured the production of

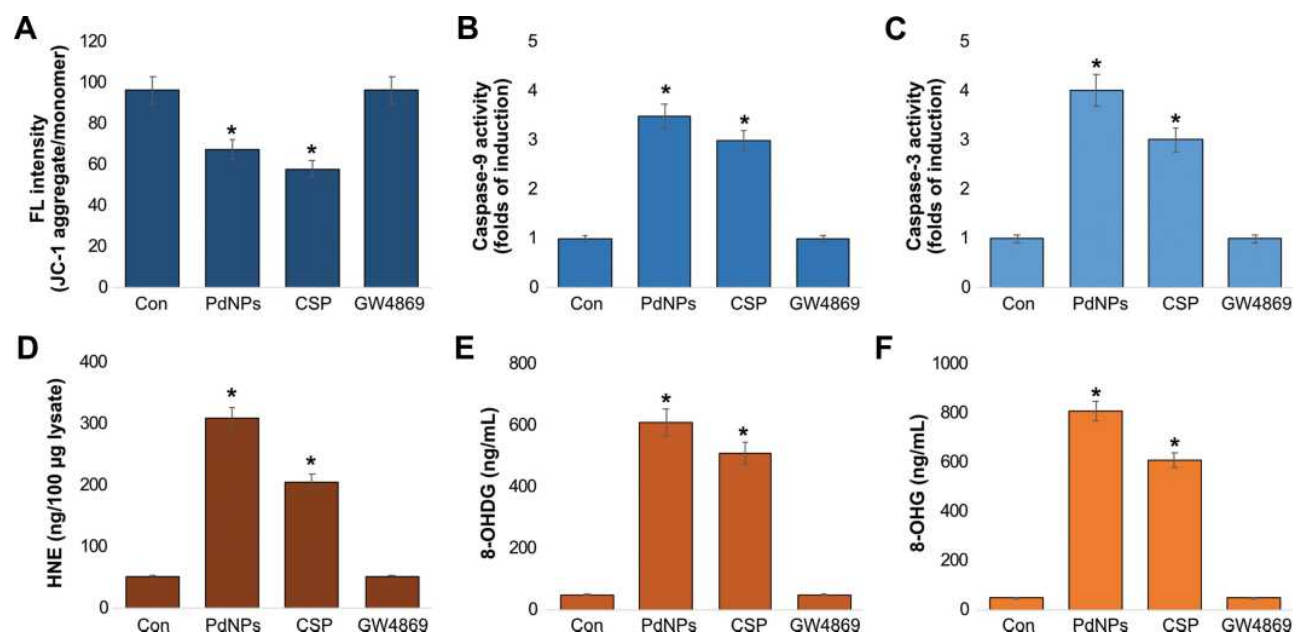


Figure 8 Effect of PdNPs on MMP, caspase 9/3, HNE, 8-OHdG, and 8-OHG in THP-1 cells. THP-1 cells were treated with PdNPs (15 μM), CSP (10 μM), or GW4869 (20 μM) in RPMI-1640 cell culture medium supplemented with 1% FCS for 24 h. Levels of (A) MMP, (B) caspase-9, (C) caspase-3, (D) HNE, (E) 8-Oxo-dG, and (F) 8-Oxo-G were determined. The results are expressed as the mean \pm standard deviation of three independent experiments. The treated groups showed statistically significant differences from the control group by the Student's *t*-test; **p* < 0.05 was considered significant.

4-HNE- in THP-1 cells treated with PdNPs. Compared to control, THP-1 cells exposed to PdNPs showed a significant increase in the levels of 4-HNE up to 300 ng (Figure 8D). Similarly, CSP-exposed THP-1 cells showed significant levels of 4-HNE up to 200 ng. Conversely, the cells treated with GW4869 for 24 h did not show a significant difference in 4-HNE relative to that in the control. Paciorek et al reported that the Hep G2 cell line increases the level of 4-HNE depending on AgNP-induced oxidative stress and affects the metabolic state of the cell. These results suggest that the production of toxic peroxidized lipids in response to PdNPs induces the production of 4-HNE.⁸⁵

Additionally, 8-OHdG and 8-OHG are the predominant forms of free radical-induced oxidative lesions and serve as biomarkers for oxidative stress and carcinogenesis. These two molecules are crucial markers for measuring the effect of endogenous oxidative damage to DNA. The estimation of these biomarkers is used to estimate DNA damage in cells. Guanine is mostly susceptible to oxidative stress. Hence, we aimed to measure the levels of 8-OHdG and 8-OHG in PdNP-exposed THP-1 cells. THP-1 cells were treated with PdNPs (15 μ M), CSP (10 μ M), or GW4869 (20 μ M) for 24 h, and cells treated with PdNPs and CSP had an 8-OHdG accumulation rate of up to 600 and 500 ng/mL, respectively, which were significantly higher than that of the control, whereas GW4869-treated cells had no accumulation (Figure 8E). Similarly, THP-1 cells treated with PdNPs and CSP had an 8-OHG accumulation rate of up to 800 and 600 ng/mL, respectively, which were significantly higher than that in the control group, whereas GW4869-treated cells showed no accumulation of 8-OHdG (Figure 8F). PdNPs have been shown to induce DNA damage in human adenocarcinoma cells (A375)¹¹⁶ and in Rat-1 and A549 cell lines.⁷² Di Guglielmo et al reported that BALB/c 3T3 fibroblast cells treated with gold nanoparticles increased the accumulation of 8-OHdG.¹¹⁷ Other metal nanoparticles such as AgNPs and TiO₂ increase the accumulation of both 8-OHdG and 8-OHG and cause DNA damage in embryonic fibroblast cells of mice and HEK-293 cells, respectively.^{77,118} Platinum nanoparticles and a combination of platinum nanoparticles and doxorubicin induced the accumulation of 8-OHdG and 8-OHG in osteosarcoma cancer cells and human monocytic THP-1 cells.^{40,92} Recently, we reported that cells exposed to PdNPs and MLT separately and cells exposed to a combination of PdNPs and MLT exhibited severe oxidative damage to both DNA and RNA through the accumulation of 8-OHdG and 8-OHG in human lung epithelial adenocarcinoma cell lines A549 and H1229.³⁸ These findings suggest that PdNPs

potentially induce mitochondrial dysfunction, caspase9/3 activation, increased 4-HNE levels, and accumulation of OHdG and 8-OHG. All these factors ultimately cause DNA damage and cell death.

PdNPs Increase AChE Activity, n-Sphingomyelinase Activity, and Exosomes Counts

Thus far, the results obtained from the above experiments indicate that oxidative stress plays a critical role in various cellular functions. Similarly, oxidative stress plays a significant role in the increased yield of exosomes. AChE activity has been developed as a marker for extracellular vesicles, which can be assayed easily, rapidly, and economically. The level of AChE activity determines the quantity of exosomes in culture supernatants or sera because AChEs are localized in the membranes of exosomes.⁵¹ To determine the expression of AChE activity, THP-1 cells were treated with PdNPs (15 μ M), CSP (10 μ M), or GW4869 (20 μ M) for 24 h, and AChE activity was subsequently analyzed. Our results suggest that PdNPs increase AChE activity up to 60 U/mL, as the cells treated with CSP increased AChE activity up to 40 U/mL (Figure 9A). Interestingly, AChE activity in cells treated with GW4869 was remarkably lower than that in PdNPs and CSP-treated cells, which was less than that found in the control cells. Ibrahim et al have reported that low concentrations of carbon nanoparticles increase AChE activity compared to high carbon nanoparticle concentrations.¹¹⁹ The oxidative stress induced by PdNPs decreases cell viability and cell proliferation of THP-1 cells; however, it induces AChE activity, which is similar to a previous report. Pérez-Aguilar et al reported that decreased levels of cell proliferation led to increased levels of AChE activity, which was associated with the down-regulation of p27 and cyclins, indicating that AChE has a tumor suppressor role in the hepatocellular carcinoma cell line.⁶⁸ AChE can induce apoptosis through the termination of cell cycle progression by facilitating apoptosome assembly and eventually induce apoptosis.^{120–122} Our findings suggest that PdNPs increase AChE activity through oxidative stress-induced apoptosis. Comprehensively, the findings from these studies suggest the possibility of increasing levels of AChE activity through oxidative stress and apoptosis induced by PdNPs.

Sphingomyelinases hydrolyze sphingomyelin into phosphorylcholine and ceramide. Ceramide regulates various

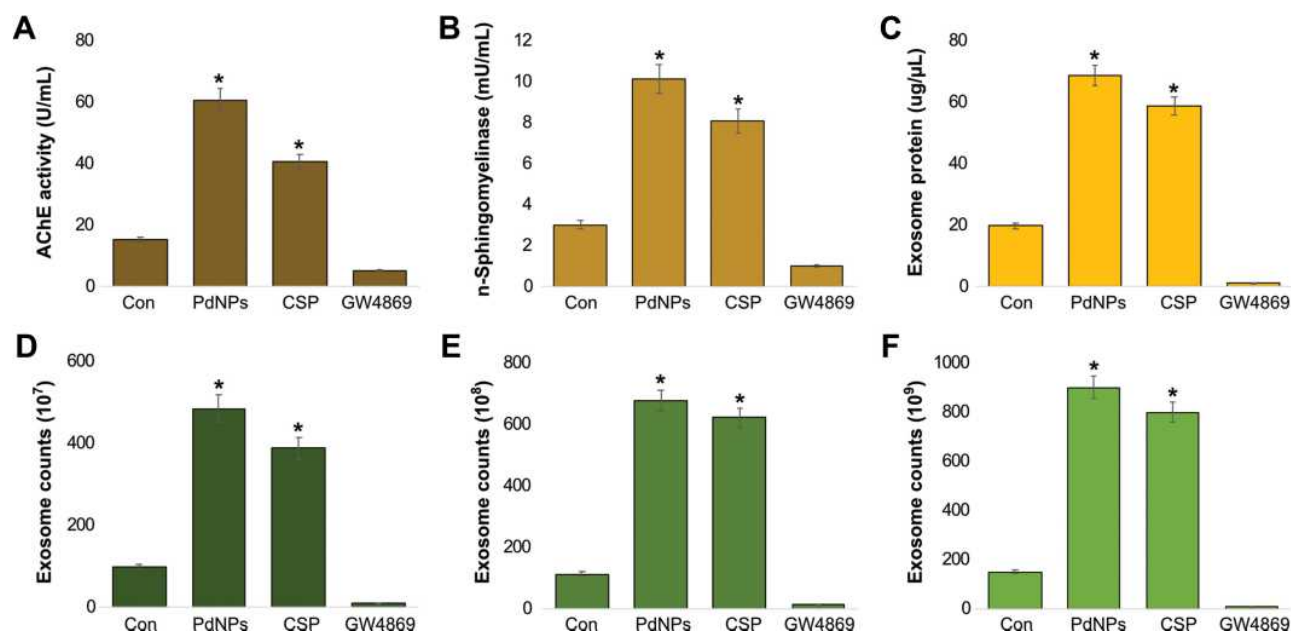


Figure 9 Effect of PdNPs on AChE activity, neutral sphingomyelinase activity, exosomal protein level, and exosome count. THP-1 cells were treated with PdNPs (15 μ M), CSP (10 μ M), or GW4869 (20 μ M) in RPMI-1640 cell culture medium supplemented with 1% FCS for 24 h. (A) AChE activity was determined from isolated exosomes using a colorimetric method. (B) Neutral sphingomyelinase activity was estimated using the Amplex Red sphingomyelinase assay kit. (C) Total protein concentration of exosomes was determined using BCA. (D) Exosomes were isolated by ExoQuick and exosomes counts were determined fluorescence polarization. (E) Exosomes were isolated by ExoQuick and exosomes counts were determined by NTA. (F) Exosomes were isolated by ExoQuick and exosomes counts were determined by EXOCET. The results are expressed as the mean \pm standard deviation of three independent experiments. The treated groups showed statistically significant differences from the control group by the Student's *t*-test; **p* < 0.05 was considered significant.

physiological processes such as growth, proliferation, apoptosis, and EV biogenesis. In addition, inhibition of n-sphingomyelinases by GW4869 potentially reduces biogenesis and secretion of EVs by blocking the ceramide-dependent budding of ILVs into the lumen of MVBs.¹²³ However, the effect of PdNPs on the involvement of n-sphingomyelinases on biogenesis and release of exosomes in THP-1 cells has not yet been explored. To determine the influence of PdNPs on n-sphingomyelinase-mediated exosome biogenesis and release, THP-1 cells were treated with PdNPs (15 μ M), CSP (10 μ M), or GW4869 (20 μ M) for 24 h. Results showed that both PdNPs and CSP increased n-sphingomyelinase activity compared to the control (Figure 9B). The cells treated with GW4869 (20 μ M) significantly decreased sphingomyelinase activity. These findings suggest that PdNPs either directly or indirectly involve the activation of sphingomyelinase, which is a possible factor involved in exosome release via the control of exosome budding into multivesicular endosomes.^{123,124} Oxidative stress increases the activity of sphingomyelinases through posttranslational modification, and sphingomyelinase play a critical role in the development of apoptosis and organ failure in sepsis.¹²⁵ Alessenko et al¹²⁶ reported that activation of n-sphingomyelinase in mice liver and brain coincided in time with increased levels of peroxide products and also ceramide

induced peroxide oxidation. Further, several studies have shown that various cellular stresses play critical roles in EV production, number, activity, composition, surface, and intravesicular proteins.^{2,26–29} Hence, oxidative stress induces n-sphingomyelinases, which are mostly involved in the biogenesis and release of vesicles.

According to previous experiments, increased levels of n-sphingomyelinases could increase the level of exosomes, and the protein concentration of exosomes directly correlated with the number of exosomes. PdNPs induce oxidative stress, activate caspases, leading to apoptosis, and eventually lead to cell death.^{37,59,60} Hence, we examined the influence of PdNPs on the total protein concentration of exosomes. First, THP-1 cells were treated with PdNPs (15 μ M), CSP (10 μ M), or GW4869 (20 μ M) for 24 h. We then isolated exosomes and quantified the protein concentration. Our results showed that compared to the control, PdNPs and CSP increased the total protein concentration of exosomes up to 70 μ g/ μ L and 60 μ g/ μ L, respectively. Additionally, THP-1 cells treated with GW4869 had a significant effect on protein concentration (Figure 9C), and the concentration of protein was dramatically reduced compared to that of the control. These findings suggest that oxidative stress and lipid peroxidation increase the

quantity of exosomes, indicating that the number of exosomes may increase in PdNP-treated cells.

The activation of AChE and n-sphingomyelinase activities as well as increasing protein concentration of exosomes support the hypothesis that PdNPs could potentially induce the number of exosomes. To further validate these results, exosomes were isolated using ExoQuick from THP-1 cells grown 1% serum condition and then the concentration of exosomes were determined using various methods including fluorescence polarization (Figure 9D), NanoTrack (Figure 9E), and EXOCET (Figure 9F). The exosomes data suggest that the quantity of exosomes significantly higher in ExoQuick method compared to ultracentrifugation. Hence, further experiments were carried out in exosomes derived from ExoQuick. All these methods consistently indicated that there was a significant increase in the number of exosomes in PdNPs and CSP-treated cells compared to that in the control cells. In contrast, cells treated with GW4869 showed significant decrease in the number of exosomes compared to that in the control. Among all the test methods, including fluorescence polarization, NanoTrack and EXOCET, for quantification of exosomes, EXOCET displayed more sensitivity, is dependable, and exhibits a high number of exosome counts. It seems to be a better method than other techniques. The promotion of exosomes is governed by the cytoskeletal regulatory protein cortactin,¹²⁷ and various types of stresses including hypoxia,²¹ acidosis,¹²⁸ thermal and oxidative stress,³¹ cytotoxic drugs,¹²⁹ and CSP.¹³⁰ Oxidative stress increases exosome secretion from retinal pigment epithelial cells, while adipocytes exposed to lipotoxic stress show enhanced release of extracellular vesicles.¹³¹ Collectively, PdNPs-induced oxidative stress could be a possible mechanism for the increased number and release of exosomes in THP-1 cells.

Size, Size Distribution, and Surface Morphology Analyses of Exosomes

DLS and nanoparticle tracking analysis (NTA) are used to measure dispersed particles in a liquid as a function of Brownian motion and to characterize isolated exosomes, which are membrane vesicles with cell diameters of approximately 20–150 nm. It provides a high-throughput and fully repeatable measurement methodology for isolated exosome particles in solution, thereby confirming their particle size and concentration. To analyze the size distribution of exosomes, we isolated exosomes from THP-1 cells exposed to

PdNPs (15 μ M), CSP (10 μ M), or GW4869 (20 μ M) for 24 h, and the size distribution of exosomes was analysed by DLS and the results were found to be 60, 50, and 60 nm, respectively, whereas the size distribution of exosomes by NTA was found to be 80, 70, and 80 nm, respectively (Figure 10A and Supplementary Figure 2). When examined with conventional SEM, the surfaces of exosomes appeared homogeneously spherical in shape in both treated and control cells (Figure 10B). The number of exosomes significantly agreed with the data obtained from fluorescence polarization, NanoTrack, and EXOCET. These results indicated that the cells treated with PdNPs and CSP showed numerous exosomes compared to those in the control group.

TEM was performed to confirm the results obtained from DLS and NTA for the presence of exosomes in both control and treated samples. While observing all micrographs, exosomes were surrounded by a single lipid bilayer. The diameter of the exosomes ranged from 30 to 60 nm (Figure 10C). They were uniformly distributed and sometimes formed aggregations or were present in the form of single vesicles. In most of the tested samples, the exosomes were spherical in shape. TEM microscopic images of both control and treated groups from various samples exhibited a high number of exosomes in treated compared to control cells, which shed a low number of EVs (Figure 10C), consistent with previous reports that control cells do not shed EVs in high proportions as compared to treated cell types.¹³² In contrast, THP-1 cells released exosomes approximately 5–6 folds. Cytostatic-, heat-, and oxidative stress-induced alterations have been reported in B16F1 mouse melanoma cell-derived small EVs.¹³³ Ag-TiO₂ nanoparticles increased the number of exosomes in B16F1 mouse melanoma cells through oxidative stress. Chemo or radiotherapy has also been shown to increase the amount of circulating tumor-derived EVs.^{134,135} Additionally, chemotherapeutic agents such as paclitaxel and doxorubicin enhance the production of pro-metastatic breast cancer-derived EVs.¹³⁶ Collectively, PdNP-induced oxidative stress plays a critical role in enhancing the level of exosome biogenesis and release. The possibility of increasing exosome release entails that cells might communicate with neighboring cells about intracellular stress.

mRNA and Protein Expression Levels of TSG101, CD9, CD63, and CD81

To corroborate the results obtained from protein quantification and total exosomes, we analyzed the expression

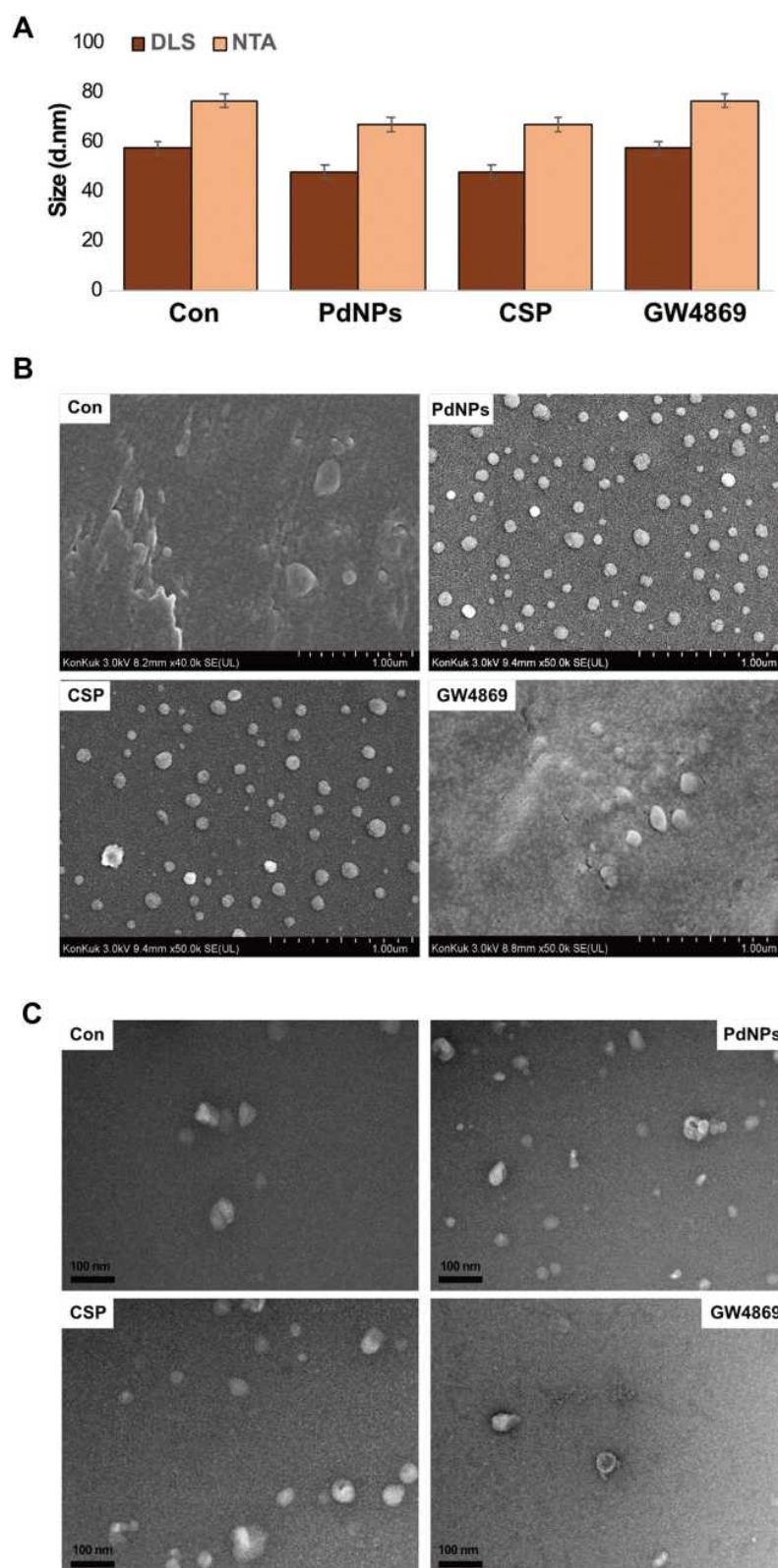


Figure 10 Size, size distribution, and morphological analyses of exosomes. THP-I cells were treated with PdNPs (15 μ M), CSP (10 μ M), or GW4869 (20 μ M) in RPMI-1640 cell culture medium supplemented with 1% FCS for 24 h. **(A)** Size distribution of exosomes was determined using DLS and NTA. **(B)** SEM images of exosomes. **(C)** TEM images of exosomes. At least three independent experiments were performed for each sample, and reproducible results were obtained.

patterns of typical exosome markers such as TSG101, CD9, CD63, and CD81 using qRT-PCR. THP-1 cells were treated with PdNPs (15 μ M), CSP (10 μ M), or GW4869 (20 μ M) for 24 h. THP-1 cells treated with PdNPs (15 μ M) or CSP (10 μ M) exhibited significantly increased expression levels of exosome markers, including TSG101, CD9, CD63, and CD81, when compared to control cells. Compared to the expression of corresponding markers in the control cells, that of these in PdNP-treated cells increased by five-, four-, six-, and six-fold, respectively, whereas that of those in CSP-treated cells increased by four-, six-, three-, and five-fold. Conversely, GW4869-treated THP-1 cells exhibited very low levels of mRNA expression compared to that in the control cells (Figure 11-upper panel). These results suggest that the exosomes released from THP-1 cells also carry information at the mRNA level, which can be helpful in understanding cancer prevention and therapy.¹³⁷

Next, we measured the expression levels of TSG101 and tetraspanin (CD9, CD63, and CD81) using ELISA. Our results showed increased expression of TSG101, CD9, CD63, and CD81 in the exosomes released from PdNPs- and CSP-treated THP-1 cells compared to that of these in the control cells. The expression of these exosomal proteins confirmed the release of exosomes from THP-1 cells. These observations support that PdNPs potentially induce exosome

secretion. The expression levels of TSG101, CD63, CD81, and CD9 in PdNP-treated cells increased by five-, six-, six-, and ten-fold, respectively, whereas their expression levels in CSP-treated cells increased by seven-, six-, six-, and six-fold, respectively, compared to that of these in the control cells. In contrast, THP-1 cells treated with GW4869 exhibited very low levels of protein expression compared to that in the control (Figure 11, lower panel). For example, low-serum condition-induced cytotoxic stress enhances the expression of PDC61/Alix, CD9, and TSG101 compared to the induction by high serum condition.¹⁹ Results from qRT-PCR and ELISA showed that the expression levels of exosome markers were higher and significant in PdNP-treated group compared with those in the control group. The mRNA and protein levels of TSG101, CD63, CD81, and CD9 were upregulated in PdNP-treated group compared with those in other groups. These data suggest that THP-1 cells have the ability to release exosomes carrying TSG101, CD63, CD81, and CD9 in the presence of PdNPs. Further, we analysed the expression of TSG101 and CD63 by Western blot. The results showed that the expression of TSG101 and CD63 were significantly high expression was observed in PdNPs and CSP treated cells compared to either GW4869 treated or control (Supplementary Figure 3). Altogether, all these findings suggest that PdNPs potentially increase the expression of exosome markers in THP-1 cells.

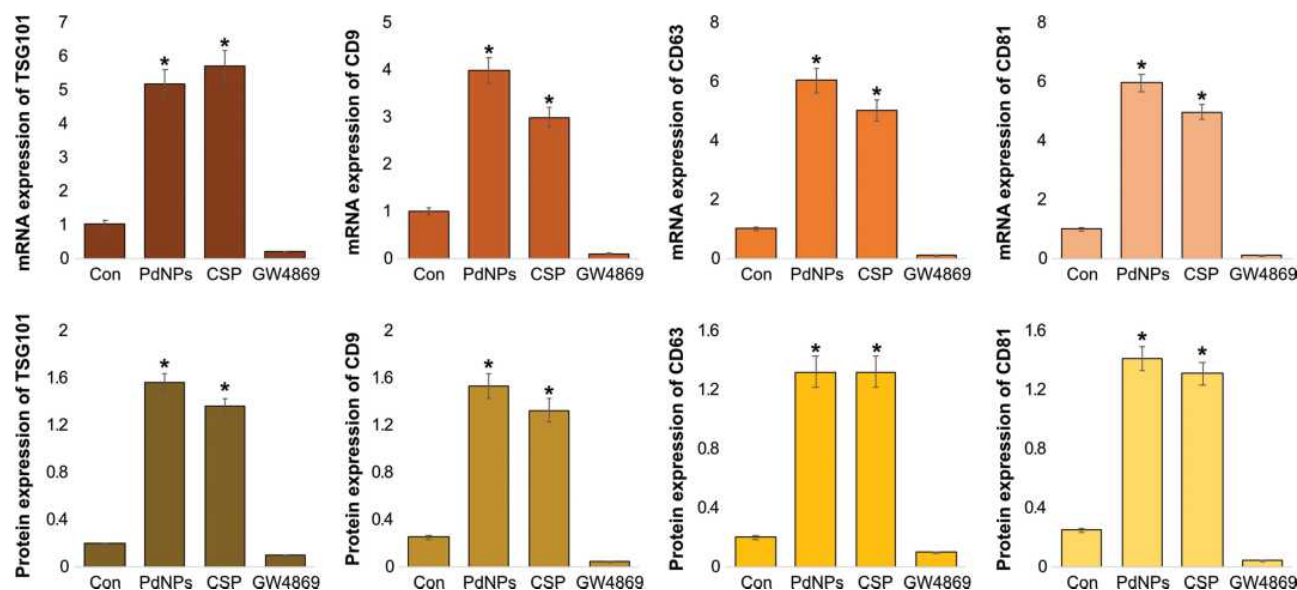


Figure 11 mRNA and protein expression levels of exosomal markers TSG101, CD81, CD63, and CD9. THP-1 cells were treated with PdNPs (15 μ M), CSP (10 μ M), or GW4869 (20 μ M) in RPMI-1640 cell culture medium supplemented with 1% FCS for 24 h. (A) The mRNA (upper panel) and (B) protein (lower panel) expression levels of TSG101, CD81, CD63, and CD9 were analyzed using ELISA. The results are expressed as the mean fold change \pm standard deviation from three independent experiments. The treated groups showed statistically significant differences from the control group by the Student's *t*-test; **p* < 0.05 was considered significant.

NAC and GW4869 Decrease PdNPs-Induced AChE Activity, n-Sphingomyelinase Activity, Exosomal Protein Count, and Exosome Count

Lipid-anchored AChE-E is a marker of reticulocytes and erythrocytes of EVs.^{138,139} Studies have reported higher AChE-E enzyme activity in “nanovesicles” pelleted at $100,000 \times g$ compared with that in microvesicles pelleted at $16,000 \times g$ or bulk plasma membrane.^{140,141} Therefore, we investigated the effect of NAC and GW4869 on the influence of PdNPs on AChE activity. THP-1 cells were treated with PdNPs (15 μ M), CSP (10 μ M), or GW4869 (20 μ M) for 24 h, and AChE activity was determined. PdNPs and CSP increased the activity of AChE compared to that in the control, whereas THP-1 cells pre-treated with NAC or GW4869 showed decreases in the activity of AChE, which was equal to that observed in the control (Figure 12A). Essandoh et al have also reported that

lipopolysaccharide induces several folds of AChE activity, which could be associated with the exosome membrane. When macrophages were pre-treated with 10 μ M GW4869, a 22% reduction in AChE activity was observed.⁵¹ Metal nanoparticles, such as silver nanoparticles, dose-dependently inhibited AChE activity in ZebraFish larvae.^{51,142}

Next, we examined the impact of NAC and GW4869 on n-sphingomyelinase activity in PdNPs (15 μ M)-, CSP (10 μ M)-, or GW4869 (20 μ M)-exposed THP-1 cells. PdNP- and CSP-treated cells showed 6- and 5-fold increases in n-sphingomyelinase activity, respectively. In contrast, THP-1 cells pre-treated with NAC or GW4869 showed decreases in the activity of n-sphingomyelinase, this decrease was equal to that observed in the control. Moreover, GW4869-treated cells showed no significant effect, similar to the control cells (Figure 12B). Yoshimura et al previously reported that GSH and NAC dose-dependently inhibited n-sphingomyelinase activity,¹⁴³ and Guo et al investigated the involvement of the

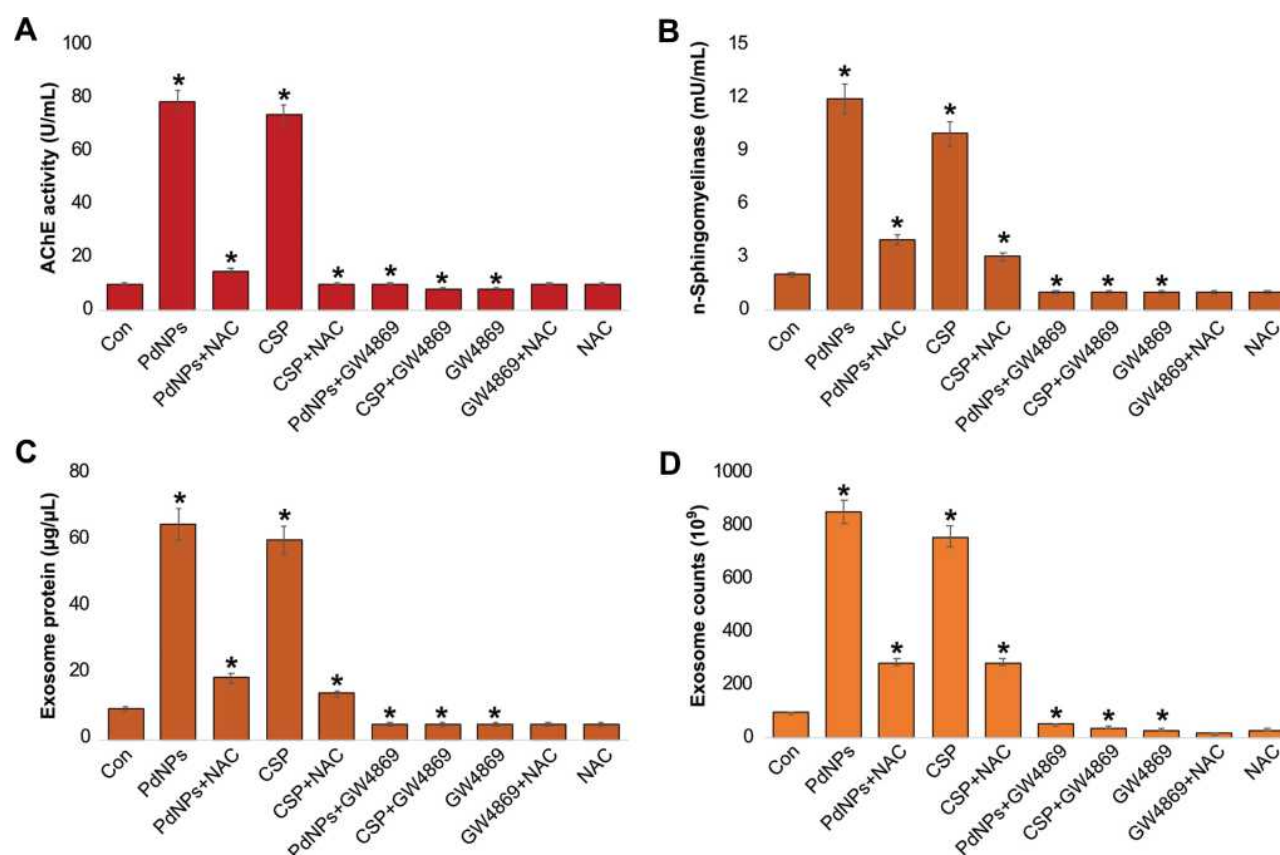


Figure 12 Effects of NAC and GW4869 on the influence of PdNPs on AChE and n-sphingomyelinase activities, exosomal protein level, and exosome count. THP-1 cells were treated with PdNPs (15 μ M), CSP (10 μ M), or GW4869 (20 μ M) in RPMI-1640 cell culture medium supplemented with 1% FCS for 24 h. The cells were pre-treated with either NAC or GW4869. (A) AChE activity was determined in exosomes using a colorimetric method. (B) Neutral sphingomyelinase activity was estimated using the Amplex Red sphingomyelinase assay kit. (C) Total protein concentration of exosomes was determined using BCA. (D) Exosome counts were determined by EXOCET. The results are expressed as the mean fold change \pm standard deviation from three independent experiments. The treated groups showed statistically significant differences from the control group by the Student's *t*-test; **p* < 0.05 was considered significant.

n-sphingomyelinase pathway in exosome biogenesis and packaging of Prion protein into vesicles.¹⁴⁴ Inhibition of this pathway using GW4869 demonstrated that n-sphingomyelinase plays a critical role in both exosome formation and PrP packaging. Further studies reported that the knockdown of n-sphingomyelinase 1 and n-sphingomyelinase 2 in mouse neurons decreased exosome release. Back et al¹⁴⁵ reported that starvation activates n-sphingomyelinase 2 and regulates autophagy and increases ceramide formation in the Golgi apparatus. Bioglass ion products could significantly promote exosome biogenesis and release from mesenchymal stem cells (MSCs) via the enhancement of the n-sphingomyelinase and Rab GTPases pathways.¹⁴⁶ Our findings suggest that Pd ions could activate n-sphingomyelinases either by oxidative stress, apoptosis, or serum starvation, and that these pathways regulate the biogenesis and release of exosomes.

Further, to corroborate the increased level of AChE and n-sphingomyelinase activities, we measured the total protein concentration of exosomes and exosome counts. As expected, THP-1 cells treated with PdNPs (15 μ M) or CSP (10 μ M) increased both total protein concentration and exosome counts, whereas cells treated with GW4869 (20 μ M) significantly decreased these parameters. In addition, there was a significant difference in exosome protein concentration and counts between the control and the GW4869- or NAC-treated THP-1 cells. Similarly, THP-1 cells pre-treated with NAC or GW4869 showed decreased total protein concentration and exosome counts (Figure 12C and D). These indicate that NAC and GW4869 are critically involved in the biogenesis and release of exosomes via the suppression of oxidative stress induced by Pd ions and n-sphingomyelinase activity by GW4869. Reductions in both exosome protein concentration and counts were possibly due to the decreased levels of n-sphingomyelinase activity and oxidative stress. Collectively, these findings suggest that PdNPs induce exosome biogenesis and release through the induction of oxidative stress and simultaneous activation of n-sphingomyelinase activity, which has significant importance in ceramide formation, triggering the budding of exosome vesicles into multivesicular bodies.¹²³

PdNPs-Induced Secreted Exosomes Contain Elevated Levels of Cytokines

Cytokines secreted by macrophages play a crucial role both in inflammation progression and immune state.¹⁴⁷ Cytokines may be packaged into EVs, and the packaging of cytokines into EVs, along with their ultimate secretion,

may also be regulated by cytokines.¹⁴⁸ Hence, to examine the influence of PdNPs on inflammatory responses through exosomes, exosomes were isolated from THP-1 cells treated with PdNPs (15 μ M), CSP (10 μ M), or GW4869 (20 μ M) for 24 h, and cytokine levels were determined using the 13-plex human suspension cyto/chemokine assay kit multiplex ELISA. The expression level of each cytokine is different from each other. We found that the expression levels of cytokines were significantly elevated in exosomes isolated from PdNP-treated or CSP-treated cells; however, PdNPs induced stronger expression than that of CSP. In contrast, GW4869-treated cells exhibited significantly lower cytokine expression levels than those in the control cells. In general, the levels of all tested pro-inflammatory cytokines in the treated groups were higher than those in the control group. The relative concentrations of IL-1 β , TNF- α , GM-CSF, IL-8, and IL-6 and MCP-1 were 300, 400, 400, 500, 1500, and 600 pg/mL, respectively, in PdNP-exposed cells, whereas they were 250, 370, 360, 500, 1300, and 500 pg/mL in CSP-exposed cells. In contrast, the relative concentrations of IL-1 β , TNF- α , GM-CSF, IL-8, IL-6, and MCP-1 were 30, 50, 50, 20, 20, and 20 pg/mL, respectively, in GW4869-treated cells. Among all levels of cytokines tested, IL-6 level was significantly higher, followed by MCP-1, IL-8, GM-CSF, TNF- α , and IL-1 β (Figure 13). Bretz et al previously found that body fluid exosomes promote the secretion of inflammatory cytokines such as IL1 β , TNF - α , and IL-6 in monocytic cells via Toll-like receptor signaling.¹⁴⁹ Tumor-derived exosomes have also been reported to trigger the release of cytokines, including IL-6, TNF- α , and TGF- β , in human blood monocytes,¹⁵⁰ and exosomes derived from RAW 264.7 mouse macrophages stimulated with LPS showed increased levels of ten different cytokines.¹⁵¹ IL-6 is one of the critical cytokines in the tumor microenvironment and is highly expressed in most cancers. This cytokine can regulate almost all hallmarks of cancer and is involved in multiple signaling pathways. These findings suggest that PdNPs potentiate increased levels of cytokine secretion from exosomes and that these cytokines could act as extracellular ligands for specific membrane receptors present on responsive target cells. The increase yield of exosomes can be used in various applications. For example, cellular-nanoporation method produced large quantities of exosomes containing therapeutic mRNAs and targeting peptides. In orthotopic phosphatase and tensin homologue (PTEN)-deficient glioma mouse models displayed mRNA-containing exosomes restored tumour-suppressor function,

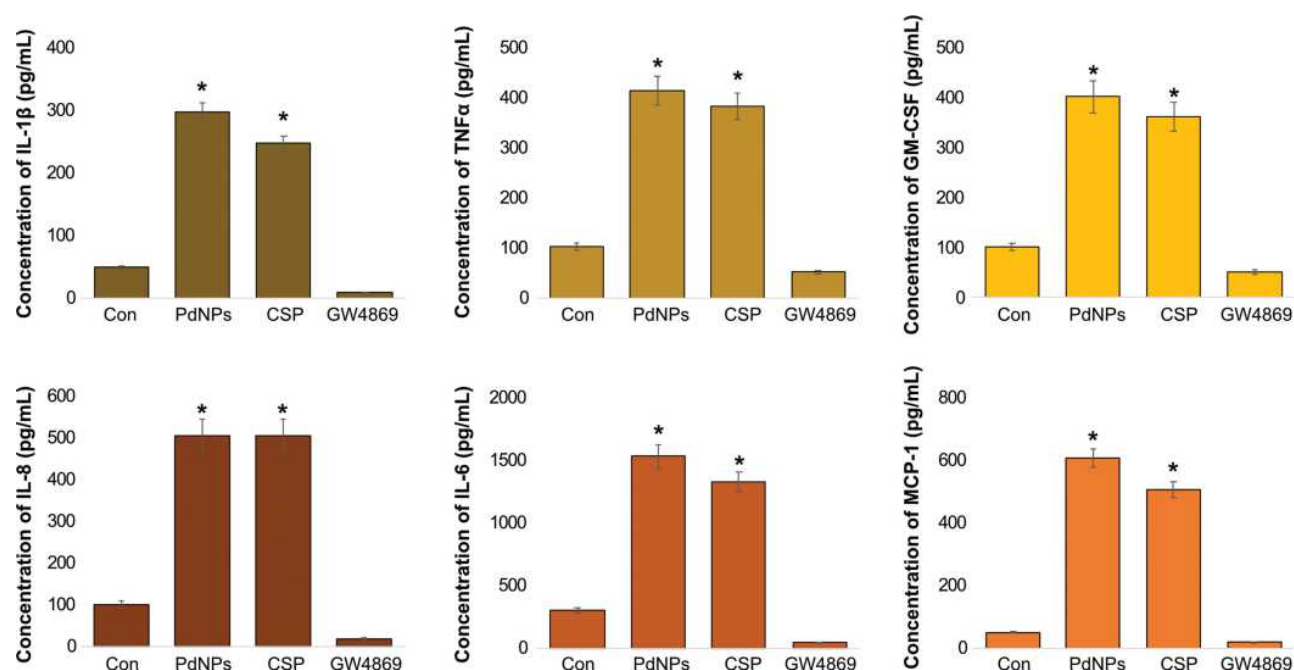


Figure 13 Effects of PdNPs on pro-inflammatory cytokines and chemokines. The expression levels of IL-1 β , TNF- α , GM-CSF, IL-8, IL-6, and MCP-1 were measured in exosomes isolated from THP-1 cells exposed to PdNPs (15 μ M), CSP (10 μ M), or GW4869 (20 μ M) in RPMI-1640 cell culture medium supplemented with 1% FCS for 24 h. The results are expressed as the mean \pm standard deviation of three independent experiments. The treated groups showed statistically significant differences from the control group by the Student's t-test; *p < 0.05 was considered significant.

enhanced inhibition of tumour growth and increased survival.¹⁵² Bioinspired exosomes are effective and safe materials, which are significantly utilized in various applications such as therapeutics and delivery and cancer immunotherapy.^{153,154} Previously, a study demonstrated sulfoxazole can inhibit the secretion of small extracellular vesicles in breast cancer cells by targeting the endothelin receptor A. Mouse model of breast cancer xenografts showed sulfoxazole reduced expression of proteins involved in biogenesis and secretion of sEV.¹⁵⁵ Collectively, PdNPs induced oxidative stress is one of the possible factors to increase biogenesis and release of exosomes.

Conclusion

To our knowledge, this is the first study demonstrating that PdNPs induce THP-1 cells to release exosomes. We evaluated the effects of PdNPs on the biogenesis and release of exosomes in THP-1 cells and found that treatment of THP-1 cells with PdNPs significantly increased exosome production by multiple folds. The released exosomes were characterized via DLS, NTA system, SEM, TEM, EXOCETTM assay, and FP. The expression of exosome markers was analyzed by qRT-PCR and ELISA. The levels

of released exosomes strongly correlated with oxidative stress, endoplasmic reticulum stress, apoptosis, and immunomodulation. The mechanism of exosome biogenesis and release possibly involves AChE and n-sphingomyelinase, which played critical roles in PdNP-treated cells, enhancing cell exosome production. In addition, we demonstrated enhanced exosome biogenesis and release by the analysis of exosomes via a series of assays, including measuring total protein concentration, exosome counts, and expression levels of TSG101, CD9, CD63, and CD81. Interestingly, NAC and GW4869 suppress PdNP-induced AChE activity, n-sphingomyelinase activity, exosomal protein level, and exosome count; all these results indicate that PdNPs indeed modulate oxidative stress and ceramide pathways, which play critical roles in the biogenesis and release of exosomes. GW4869 not only decreased PdNP-promoted exosome count but also the levels of cytokines and chemokines in the exosomes of THP-1 cells. Exosomes obtained from THP-1 cells could be used for therapeutic benefits by attenuating or stimulating immune response. Thus, PdNPs could be used to enhance exosome secretion from THP-1 cells for practical application, which could be a useful strategy to increase exosome yield. However, further studies are necessary to find out

the precise mechanism of PdNP-mediated elevation of exosome production.

Acknowledgments

This paper was supported by Konkuk University in 2019.

Funding

This paper was funded by Konkuk University in 2019.

Disclosure

The authors declare no conflicts of interest.

References

- Hao T, Li-Talley M, Buck A, Chen W. An emerging trend of rapid increase of leukemia but not all cancers in the aging population in the United States. *Sci Rep*. 2019;9(1):12070. doi:10.1038/s41598-019-48445-1
- Kowal J, Arras G, Colombo M, et al. Proteomic comparison defines novel markers to characterize heterogeneous populations of extracellular vesicle subtypes. *Proc Natl Acad Sci U S A*. 2016;113(8):E968–E977. doi:10.1073/pnas.1521230113
- Tricarico C, Clancy J, D'Souza-Schorey C. Biology and biogenesis of shed microvesicles. *Small GTPases*. 2017;8(4):220–232. doi:10.1080/21541248.2016.1215283
- Atkin-Smith GK, Poon IKH. Disassembly of the dying: mechanisms and functions. *Trends Cell Biol*. 2017;27(2):151–162. doi:10.1016/j.tcb.2016.08.011
- Yang B, Chen Y, Shi J. Exosome biochemistry and advanced nanotechnology for next-generation theranostic platforms. *Adv Mater*. 2019;31(2):e1802896. doi:10.1002/adma.201802896
- Simons M, Raposo G. Exosomes – vesicular carriers for intercellular communication. *Curr Opin Cell Biol*. 2009;21(4):575–581. doi:10.1016/jceb.2009.03.007
- Mathivanan S, Lim JW, Tauro BJ, Ji H, Moritz RL, Simpson RJ. Proteomics analysis of A33 immunoaffinity-purified exosomes released from the human colon tumor cell line LIM1215 reveals a tissue-specific protein signature. *Mol Cell Proteomics*. 2010;9(2):197–208. doi:10.1074/mcp.M900152-MCP200
- Gross JC, Chaudhary V, Bartscherer K, Boutros M. Active Wnt proteins are secreted on exosomes. *Nat Cell Biol*. 2012;14(10):1036–1045. doi:10.1038/ncb2574
- Zhang Y, Liu Y, Liu H, Tang WH. Exosomes: biogenesis, biologic function and clinical potential. *Cell Biosci*. 2019;9(1):19. doi:10.1186/s13578-019-0282-2
- Minciacchi VR, Freeman MR, Di Vizio D. Extracellular vesicles in cancer: exosomes, microvesicles and the emerging role of large oncosomes. *Semin Cell Dev Biol*. 2015;40:41–51. doi:10.1016/j.semcdb.2015.02.010
- Sahu R, Kaushik S, Clement CC, et al. Microautophagy of cytosolic proteins by late endosomes. *Dev Cell*. 2011;20(1):131–139. doi:10.1016/j.devcel.2010.12.003
- Villarroya-Beltri C, Baixauli F, Gutiérrez-Vázquez C, Sánchez-Madrid F, Mittelbrunn M. Sorting it out: regulation of exosome loading. *Semin Cancer Biol*. 2014;28:3–13. doi:10.1016/j.semcancer.2014.04.009
- Airola MV, Hannun YA. Sphingolipid metabolism and neutral sphingomyelinases. *Handb Exp Pharmacol*. 2013;215:57–76. doi:10.1007/978-3-7091-1368-4_3
- Castro BM, Prieto M, Silva LC. Ceramide: a simple sphingolipid with unique biophysical properties. *Prog Lipid Res*. 2014;54:53–67. doi:10.1016/j.plipres.2014.01.004
- Perez-Hernandez D, Gutiérrez-Vázquez C, Jorge I, et al. The intracellular interactome of tetraspanin-enriched microdomains reveals their function as sorting machineries toward exosomes. *J Biol Chem*. 2013;288(17):11649–11661. doi:10.1074/jbc.M112.445304
- Llorente A, van Deurs B, Sandvig K. Cholesterol regulates prosome release from secretory lysosomes in PC-3 human prostate cancer cells. *Eur J Cell Biol*. 2007;86(7):405–415. doi:10.1016/j.ejcb.2007.05.001
- Koumangoye RB, Sakwe AM, Goodwin JS, Patel T, Ochieng J, Srivastava RK. Detachment of breast tumor cells induces rapid secretion of exosomes which subsequently mediate cellular adhesion and spreading. *PLoS One*. 2011;6(9):e24234. doi:10.1371/journal.pone.0024234
- Phuyal S, Hessvik NP, Skotland T, Sandvig K, Llorente A. Regulation of exosome release by glycosphingolipids and flotillins. *FEBS J*. 2014;281(9):2214–2227. doi:10.1111/febs.12775
- Li J, Lee Y, Johansson HJ, et al. Serum-free culture alters the quantity and protein composition of neuroblastoma-derived extracellular vesicles. *J Extracell Vesicles*. 2015;4(1):26883. doi:10.3402/jev.v4.26883
- Savina A, Furlán M, Vidal M, Colombo MI. Exosome release is regulated by a calcium-dependent mechanism in K562 cells. *J Biol Chem*. 2003;278(22):20083–20090. doi:10.1074/jbc.M301642200
- King HW, Michael MZ, Gleadow JM. Hypoxic enhancement of exosome release by breast cancer cells. *BMC Cancer*. 2012;12(1):421. doi:10.1186/1471-2407-12-421
- Atienzar-Aroca S, Flores-Bellver M, Serrano-Heras G, et al. Oxidative stress in retinal pigment epithelium cells increases exosome secretion and promotes angiogenesis in endothelial cells. *J Cell Mol Med*. 2016;20(8):1457–1466. doi:10.1111/jcmm.12834
- Zhu L, Zang J, Liu B, et al. Oxidative stress-induced RAC autophagy can improve the HUVEC functions by releasing exosomes. *J Cell Physiol*. 2020;235(10):7392–7409. doi:10.1002/jcp.29641
- Pollet H, Conrard L, Cloos A-S, Tyteca D. Plasma membrane lipid domains as platforms for vesicle biogenesis and shedding? *Biomolecules*. 2018;8(3):94. doi:10.3390/biom8030094
- Emam SE, Ando H, Abu Lila AS, et al. A novel strategy to increase the yield of exosomes (extracellular vesicles) for an expansion of basic research. *Biol Pharm Bull*. 2018;41(5):733–742. doi:10.1248/bpb.b17-00919
- Oskowitz A, McFerrin H, Gutschow M, Carter ML, Pochampally R. Serum-deprived human multipotent mesenchymal stromal cells (MSCs) are highly angiogenic. *Stem Cell Res*. 2011;6(3):215–225. doi:10.1016/j.scr.2011.01.004
- Aubertin K, Silva AK, Luciani N, et al. Massive release of extracellular vesicles from cancer cells after photodynamic treatment or chemotherapy. *Sci Rep*. 2016;6(1):35376. doi:10.1038/srep35376
- Sun Y, Liu J. Potential of cancer cell-derived exosomes in clinical application: a review of recent research advances. *Clin Ther*. 2014;36(6):863–872. doi:10.1016/j.clinthera.2014.04.018
- Taverna S, Ghersi G, Ginestra A, et al. Shedding of membrane vesicles mediates fibroblast growth factor-2 release from cells. *J Biol Chem*. 2003;278(51):51911–51919. doi:10.1074/jbc.M304192200
- Haraszti RA, Miller R, Dubuke ML, et al. Serum deprivation of mesenchymal stem cells improves exosome activity and alters lipid and protein composition. *iScience*. 2019;16:230–241. doi:10.1016/j.isci.2019.05.029
- Hedlund M, Nagaeva O, Kargl D, Baranov V, Mincheva-Nilsson L, Zimmer J. Thermal- and oxidative stress causes enhanced release of NKG2D ligand-bearing immunosuppressive exosomes in leukemia/lymphoma T and B cells. *PLoS One*. 2011;6(2):e16899. doi:10.1371/journal.pone.0016899

32. Wang T, Gilkes DM, Takano N, et al. Hypoxia-inducible factors and RAB22A mediate formation of microvesicles that stimulate breast cancer invasion and metastasis. *Proc Natl Acad Sci U S A*. 2014;111(31):E3234–E3242. doi:10.1073/pnas.1410041111
33. Vulpis E, Cecere F, Molfetta R, et al. Genotoxic stress modulates the release of exosomes from multiple myeloma cells capable of activating NK cell cytokine production: role of HSP70/TLR2/NF- κ B axis. *Oncoimmunology*. 2017;6(3):e1279372. doi:10.1080/2162402x.2017.1279372
34. Bandari SK, Purushothaman A, Ramani VC, et al. Chemotherapy induces secretion of exosomes loaded with heparanase that degrades extracellular matrix and impacts tumor and host cell behavior. *Matrix Biol*. 2018;65:104–118. doi:10.1016/j.matbio.2017.09.001
35. Gobbo J, Marcion G, Cordonnier M, et al. Restoring anticancer immune response by targeting tumor-derived exosomes with a HSP70 peptide aptamer. *J Natl Cancer Inst*. 2016;108(3):djv330. doi:10.1093/jnci/djv330
36. Bosshart H, Heinzelmänn M. THP-1 cells as a model for human monocytes. *Ann Transl Med*. 2016;4(21):438. doi:10.21037/atm.2016.08.53
37. Gurunathan S, Kim E, Han JW, Park JH, Kim J-H. Green chemistry approach for synthesis of effective anticancer palladium nanoparticles. *Molecules*. 2015;20(12):22476–22498. doi:10.3390/molecules201219860
38. Gurunathan S, Jeyaraj M, Kang M-H, Kim J-H. Melatonin enhances palladium-nanoparticle-induced cytotoxicity and apoptosis in human lung epithelial adenocarcinoma cells A549 and H1229. *Antioxidants (Basel)*. 2020;9(4):357. doi:10.3390/antiox9040357
39. Gurunathan S, Han JW, Eppakayala V, Kim J-H. Green synthesis of graphene and its cytotoxic effects in human breast cancer cells. *Int J Nanomedicine*. 2013;8:1015. doi:10.2147/IJN.S42047
40. Gurunathan S, Jeyaraj M, Kang M-H, Kim J-H. The effects of apigenin-biosynthesized ultra-small platinum nanoparticles on the human monocytic THP-1 cell line. *Cells*. 2019;8(5):444. doi:10.3390/cells8050444
41. Chen Y, Rosazza JP. Purification and characterization of nitric oxide synthase (NOSNoc) from a *Nocardia* species. *J Bacteriol*. 1995;177(17):5122–5128. doi:10.1128/jb.177.17.5122-5128.1995
42. Maisonneuve E, Frayssé L, Lignon S, Capron L, Dukan S. Carbonylated proteins are detectable only in a degradation-resistant aggregate state in *Escherichia coli*. *J Bacteriol*. 2008;190(20):6609–6614. doi:10.1128/JB.00588-08
43. de Sousa Leal AM, de Queiroz JD, de Medeiros SR, de Souza Lima TK, Agnez-Lima LF. Violacein induces cell death by triggering mitochondrial membrane hyperpolarization in vitro. *BMC Microbiol*. 2015;15(1):115. doi:10.1186/s12866-015-0452-2
44. Cheng Q, Li X, Wang Y, Dong M, Zhan F-H, Liu J. The ceramide pathway is involved in the survival, apoptosis and exosome functions of human multiple myeloma cells in vitro. *Acta Pharmacol Sin*. 2018;39(4):561–568. doi:10.1038/aps.2017.118
45. Gurunathan S, Marash M, Weinberger A, Gerst JE, Schekman R. t-SNARE phosphorylation regulates endocytosis in yeast. *Mol Biol Cell*. 2002;13(5):1594–1607. doi:10.1091/mbc.01-11-0541
46. Wu M, Ouyang Y, Wang Z, et al. Isolation of exosomes from whole blood by integrating acoustics and microfluidics. *Proc Natl Acad Sci U S A*. 2017;114(40):10584–10589. doi:10.1073/pnas.1709210114
47. Lim J, Choi M, Lee H, et al. Direct isolation and characterization of circulating exosomes from biological samples using magnetic nanowires. *J Nanobiotechnology*. 2019;17(1):1. doi:10.1186/s12951-018-0433-3
48. Soares Martins T, Catita J, Martins Rosa I, AB da Cruz e Silva O, Henriques AG, Fan G-C. Exosome isolation from distinct biofluids using precipitation and column-based approaches. *PLoS One*. 2018;13(6):e0198820. doi:10.1371/journal.pone.0198820
49. Kalimuthu K, Kwon WY, Park KS. A simple approach for rapid and cost-effective quantification of extracellular vesicles using a fluorescence polarization technique. *J Biol Eng*. 2019;13(1):31. doi:10.1186/s13036-019-0160-9
50. Genneböck N, Hellman U, Malm L, et al. Growth factor stimulation of cardiomyocytes induces changes in the transcriptional contents of secreted exosomes. *J Extracell Vesicles*. 2013;2(1):20167. doi:10.3402/jev.v2i0.20167
51. Essandoh K, Yang L, Wang X, et al. Blockade of exosome generation with GW4869 dampens the sepsis-induced inflammation and cardiac dysfunction. *Biochim Biophys Acta*. 2015;1852(11):2362–2371. doi:10.1016/j.bbdis.2015.08.010
52. Tabatadze N, Savonenko A, Song H, Bandaru VV, Chu M, Haughey NJ. Inhibition of neutral sphingomyelinase-2 perturbs brain sphingolipid balance and spatial memory in mice. *J Neurosci Res*. 2010;88(13):2940–2951. doi:10.1002/jnr.22438
53. Evangelisti C, Panziera N, D'Alessio A, Bertinetti L, Botavina M, Vitulli G. New monodispersed palladium nanoparticles stabilized by poly-(N-vinyl-2-pyrrolidone): preparation, structural study and catalytic properties. *J Catal*. 2010;272(2):246–252. doi:10.1016/j.jcat.2010.04.006
54. Schiavo L, Aversa L, Tatti R, Verucchi R, Carotenuto G. Structural characterizations of palladium clusters prepared by polyol reduction of [PdCl₄]²⁻ ions. *J Anal Methods Chem*. 2016;2016:9073594. doi:10.1155/2016/9073594
55. Nadagouda MN, Varma RS. Green synthesis of silver and palladium nanoparticles at room temperature using coffee and tea extract. *Green Chem*. 2008;10(8):859–862. doi:10.1039/B804703K
56. Shen Y, Philip D, Mathew J. Rapid green synthesis of palladium nanoparticles using the dried leaf of *Anacardium occidentale*. *Spectrochim Acta A Mol Biomol Spectrosc*. 2012;91:35–38. doi:10.1016/j.saa.2012.01.063
57. Khan M, Khan M, Kuniyil M, et al. Biogenic synthesis of palladium nanoparticles using *Pulicaria glutinosa* extract and their catalytic activity towards the Suzuki coupling reaction. *Dalton Trans*. 2014;43(24):9026–9031. doi:10.1039/c3dt53554a
58. Shaik MR, Ali ZJ, Khan M, et al. Green synthesis and characterization of palladium nanoparticles using *Origanum vulgare* L. extract and their catalytic activity. *Molecules*. 2017;22(1):165. doi:10.3390/molecules22010165
59. Zhang X-F, Yan Q, Shen W, Gurunathan S. Trichostatin A enhances the apoptotic potential of palladium nanoparticles in human cervical cancer cells. *Int J Mol Sci*. 2016;17(8):1354. doi:10.3390/ijms17081354
60. Yuan Y-G, Peng Q-L, Gurunathan S. Combination of palladium nanoparticles and tubastatin-A potentiates apoptosis in human breast cancer cells: a novel therapeutic approach for cancer. *Int J Nanomedicine*. 2017;12:6503–6520. doi:10.2147/ijn.S136142
61. Gurunathan S, Qasim M, Park CH, et al. Cytotoxicity and transcriptomic analyses of biogenic palladium nanoparticles in human ovarian cancer cells (SKOV3). *Nanomaterials (Basel)*. 2019;9(5):787. doi:10.3390/nano9050787
62. Piao Y, Jang Y, Shokouhimehr M, Lee IS, Hyeon T. Facile aqueous-phase synthesis of uniform palladium nanoparticles of various shapes and sizes. *Small*. 2007;3(2):255–260. doi:10.1002/smll.200600402
63. Peng X, Cui Z, Bai X, Lv H. Bio-synthesis of palladium nanocubes and their electrocatalytic properties. *IET Nanobiotechnol*. 2018;12(8):1031–1036. doi:10.1049/iet-nbt.2018.5159
64. Hazarika M, Borah D, Bora P, Silva AR, Das P, Mishra YK. Biogenic synthesis of palladium nanoparticles and their applications as catalyst and antimicrobial agent. *PLoS One*. 2017;12(9):e0184936. doi:10.1371/journal.pone.0184936
65. Takeoka H, Fukui N, Sakurai S, Nakamura Y, Fujii S. Nanomorphology characterization of sterically stabilized polypyrrole-palladium nanocomposite particles. *Polym J*. 2014;46(10):704–709. doi:10.1038/pj.2014.44

66. Rashid M-U, Coombs KM. Serum-reduced media impacts on cell viability and protein expression in human lung epithelial cells. *J Cell Physiol.* 2019;234(6):7718–7724. doi:10.1002/jcp.27890
67. Savina A, Vidal M, Colombo MI. The exosome pathway in K562 cells is regulated by Rab11. *J Cell Sci.* 2002;115(Pt 12):2505–2515. doi:10.3410/f.11414964.12436063
68. Pérez-Aguilar B, Vidal CJ, Palomec G, et al. Acetylcholinesterase is associated with a decrease in cell proliferation of hepatocellular carcinoma cells. *Biochim Biophys Acta.* 2015;1852(7):1380–1387. doi:10.1016/j.bbdis.2015.04.003
69. McGrath AJ, Chien Y-H, Cheong S, et al. Gold over branched palladium nanostructures for photothermal cancer therapy. *ACS Nano.* 2015;9(12):12283–12291. doi:10.1021/acs.nano.5b05563
70. Antunovic M, Kriznik B, Ulukaya E, et al. Cytotoxic activity of novel palladium-based compounds on leukemia cell lines. *Anticancer Drugs.* 2015;26(2):180–186. doi:10.1097/cad.0000000000000174
71. Anand K, Tiloke C, Phulukdaree A, et al. Biosynthesis of palladium nanoparticles by using *Moringa oleifera* flower extract and their catalytic and biological properties. *J Photochem Photobiol B.* 2016;165:87–95. doi:10.1016/j.jphotobiol.2016.09.039
72. Iavicoli I, Farina M, Fontana L, et al. In vitro evaluation of the potential toxic effects of palladium nanoparticles on fibroblasts and lung epithelial cells. *Toxicol in Vitro.* 2017;42:191–199. doi:10.1016/j.tiv.2017.04.024
73. Akter N, Sadowski JT, Zhou C, et al. Morphology of palladium thin film deposited on a two-dimensional bilayer aluminosilicate. *Top Catal.* 2019;62(12–16):1067–1075. doi:10.1007/s11244-019-01193-y
74. Yu Z, Li Q, Wang J, et al. Reactive oxygen species-related nanoparticle toxicity in the biomedical field. *Nanoscale Res Lett.* 2020;15(1):115. doi:10.1186/s11671-020-03344-7
75. Zhang X-F, Choi Y-J, Han JW, et al. Differential nanoreprotoxicity of silver nanoparticles in male somatic cells and spermatogonial stem cells. *Int J Nanomedicine.* 2015;10:1335–1357. doi:10.2147/ijn.S76062
76. Han JW, Gurunathan S, Choi Y-J, Kim J-H. Dual functions of silver nanoparticles in F9 teratocarcinoma stem cells, a suitable model for evaluating cytotoxicity- and differentiation-mediated cancer therapy. *Int J Nanomedicine.* 2017;12:7529–7549. doi:10.2147/ijn.S145147
77. Gurunathan S, Qasim M, Park C, et al. Cytotoxicity and transcriptomic analysis of silver nanoparticles in mouse embryonic fibroblast cells. *Int J Mol Sci.* 2018;19(11):3618. doi:10.3390/ijms19113618
78. Gurunathan S, Raman J, Abd Malek SN, John PA, Vikineswary S. Green synthesis of silver nanoparticles using *Ganoderma neo-japonicum* Imazeki: a potential cytotoxic agent against breast cancer cells. *Int J Nanomedicine.* 2013;8:4399–4413. doi:10.2147/ijn.S51881
79. Gurunathan S, Park JH, Han JW, Kim J-H. Comparative assessment of the apoptotic potential of silver nanoparticles synthesized by *Bacillus tequilensis* and *Calocybe indica* in MDA-MB-231 human breast cancer cells: targeting p53 for anticancer therapy. *Int J Nanomedicine.* 2015;10:4203–4222. doi:10.2147/ijn.S83953
80. Han JW, Gurunathan S, Jeong J-K, et al. Oxidative stress mediated cytotoxicity of biologically synthesized silver nanoparticles in human lung epithelial adenocarcinoma cell line. *Nanoscale Res Lett.* 2014;9(1):459. doi:10.1186/1556-276x-9-459
81. Jeong JK, Gurunathan S, Kang MH, et al. Hypoxia-mediated autophagic flux inhibits silver nanoparticle-triggered apoptosis in human lung cancer cells. *Sci Rep.* 2016;6:21688. doi:10.1038/srep21688
82. Gurunathan S, Jeyaraj M, La H, et al. Anisotropic platinum nanoparticle-induced cytotoxicity, apoptosis, inflammatory response, and transcriptomic and molecular pathways in human acute monocytic leukemia cells. *Int J Mol Sci.* 2020;21(2):440. doi:10.3390/ijms21020440
83. Chapple SJ, Cheng X, Mann GE. Effects of 4-hydroxynonenal on vascular endothelial and smooth muscle cell redox signaling and function in health and disease. *Redox Biol.* 2013;1(1):319–331. doi:10.1016/j.redox.2013.04.001
84. Zhornik EV, Baranova LA, Drozd ES, et al. Silver nanoparticles induce lipid peroxidation and morphological changes in human lymphocytes surface. *Biofizika.* 2014;59(3):466–473. doi:10.1134/S0006350914030282
85. Paciorek P, Żuberek M, Grzelak A. Products of lipid peroxidation as a factor in the toxic effect of silver nanoparticles. *Materials (Basel).* 2020;13(11):2460. doi:10.3390/ma13112460
86. Teoh ML, Sun W, Smith BJ, Oberley LW, Cullen JJ. Modulation of reactive oxygen species in pancreatic cancer. *Clin Cancer Res.* 2007;13(24):7441–7450. doi:10.1158/1078-0432.Ccr-07-0851
87. Teoh-Fitzgerald ML, Fitzgerald MP, Jensen TJ, Futscher BW, Domann FE. Genetic and epigenetic inactivation of extracellular superoxide dismutase promotes an invasive phenotype in human lung cancer by disrupting ECM homeostasis. *Mol Cancer Res.* 2012;10(1):40–51. doi:10.1158/1541-7786.Mcr-11-0501
88. Gurunathan S, Kim J-H. Biocompatible gold nanoparticles ameliorate retinoic acid-induced cell death and induce differentiation in F9 teratocarcinoma stem cells. *Nanomaterials (Basel).* 2018;8(6):396. doi:10.3390/nano8060396
89. Gurunathan S, Jeyaraj M, Kang M-H, Kim J-H. Anticancer properties of platinum nanoparticles and retinoic acid: combination therapy for the treatment of human neuroblastoma cancer. *Int J Mol Sci.* 2020;21(18):6792. doi:10.3390/ijms21186792
90. Haase A, Rott S, Manton A, et al. Effects of silver nanoparticles on primary mixed neural cell cultures: uptake, oxidative stress and acute calcium responses. *Toxicol Sci.* 2012;126(2):457–468. doi:10.1093/toxsci/kfs003
91. Verano-Braga T, Miethling-Graff R, Wojdyla K, et al. Insights into the cellular response triggered by silver nanoparticles using quantitative proteomics. *ACS Nano.* 2014;8(3):2161–2175. doi:10.1021/nn4050744
92. Gurunathan S, Jeyaraj M, Kang M-H, Kim J-H. Tangeretin-assisted platinum nanoparticles enhance the apoptotic properties of doxorubicin: combination therapy for Osteosarcoma treatment. *Nanomaterials (Basel).* 2019;9(8):1089. doi:10.3390/nano9081089
93. Fahmy B, Cormier SA. Copper oxide nanoparticles induce oxidative stress and cytotoxicity in airway epithelial cells. *Toxicol in Vitro.* 2009;23(7):1365–1371. doi:10.1016/j.tiv.2009.08.005
94. Noël A, Maghni K, Cloutier Y, et al. Effects of inhaled nano-TiO₂ aerosols showing two distinct agglomeration states on rat lungs. *Toxicol Lett.* 2012;214(2):109–119. doi:10.1016/j.toxlet.2012.08.019
95. Traverso N, Ricciarelli R, Nitti M, et al. Role of glutathione in cancer progression and chemoresistance. *Oxid Med Cell Longev.* 2013;2013:972913. doi:10.1155/2013/972913
96. Gurunathan S, Arsalan Iqbal M, Qasim M, et al. Evaluation of graphene oxide induced cellular toxicity and transcriptome analysis in human embryonic kidney cells. *Nanomaterials (Basel).* 2019;9(7):969. doi:10.3390/nano9070969
97. Gurunathan S, Kang M-H, Jeyaraj M, Kim J-H. Differential immunomodulatory effect of graphene oxide and vanillin-functionalized graphene oxide nanoparticles in human acute monocytic leukemia cell line (THP-1). *Int J Mol Sci.* 2019;20(2):247. doi:10.3390/ijms20020247
98. Sengupta R, Holmgren A. The role of thioredoxin in the regulation of cellular processes by S-nitrosylation. *Biochim Biophys Acta.* 2012;1820(6):689–700. doi:10.1016/j.bbagen.2011.08.012
99. Akter M, Sikder MT, Rahman MM, et al. A systematic review on silver nanoparticles-induced cytotoxicity: physicochemical properties and perspectives. *J Adv Res.* 2018;9:1–16. doi:10.1016/j.jare.2017.10.008

100. Yuan YG, Gurunathan S. Combination of graphene oxide-silver nanoparticle nanocomposites and cisplatin enhances apoptosis and autophagy in human cervical cancer cells. *Int J Nanomedicine*. 2017;12:6537–6558. doi:10.2147/ijn.S125281
101. Niska K, Santos-Martinez MJ, Radomski MW, Inkielewicz-Stepniak I. CuO nanoparticles induce apoptosis by impairing the antioxidant defense and detoxification systems in the mouse hippocampal HT22 cell line: protective effect of crocetin. *Toxicol in Vitro*. 2015;29(4):663–671. doi:10.1016/j.tiv.2015.02.004
102. Adeyemi OS, Faniyan TO. Antioxidant status of rats administered silver nanoparticles orally. *J Taibah Univ Med Sci*. 2014;9(3):182–186. doi:10.1016/j.jtumed.2014.03.002
103. Li Y, Guo Y, Tang J, Jiang J, Chen Z. New insights into the roles of CHOP-induced apoptosis in ER stress. *Acta Biochim Biophys Sin (Shanghai)*. 2014;46(8):629–640. doi:10.1093/abbs/gmu048
104. Collett GP, Redman CW, Sargent IL, Vatish M. Endoplasmic reticulum stress stimulates the release of extracellular vesicles carrying danger-associated molecular pattern (DAMP) molecules. *Oncotarget*. 2018;9(6):6707–6717. doi:10.18632/oncotarget.24158
105. Yang X, Shao H, Liu W, et al. Endoplasmic reticulum stress and oxidative stress are involved in ZnO nanoparticle-induced hepatotoxicity. *Toxicol Lett*. 2015;234(1):40–49. doi:10.1016/j.toxlet.2015.02.004
106. Yu KN, Chang SH, Park SJ, et al. Titanium dioxide nanoparticles induce endoplasmic reticulum stress-mediated autophagic cell death via mitochondria-associated endoplasmic reticulum membrane disruption in normal lung cell. *PLoS One*. 2015;10(6):e0131208. doi:10.1371/journal.pone.0131208
107. Simard JC, Durocher I, Girard D. Silver nanoparticles induce irremediable endoplasmic reticulum stress leading to unfolded protein response dependent apoptosis in breast cancer cells. *Apoptosis*. 2016;21(11):1279–1290. doi:10.1007/s10495-016-1285-7
108. Christen V, Camenzind M, Fent K. Silica nanoparticles induce endoplasmic reticulum stress response, oxidative stress and activate the mitogen-activated protein kinase (MAPK) signaling pathway. *Toxicol Rep*. 2014;1:1143–1151. doi:10.1016/j.toxrep.2014.10.023
109. Christen V, Fent K. Silica nanoparticles induce endoplasmic reticulum stress response and activate mitogen activated kinase (MAPK) signalling. *Toxicol Rep*. 2016;3:832–840. doi:10.1016/j.toxrep.2016.10.009
110. Gurunathan S, Kang MH, Kim JH. Combination effect of silver nanoparticles and histone deacetylases inhibitor in human alveolar basal epithelial cells. *Molecules*. 2018;23(8):2046. doi:10.3390/molecules23082046
111. Choi YJ, Gurunathan S, Kim JH. Graphene oxide-silver nanocomposite enhances cytotoxic and apoptotic potential of Salinomycin in human ovarian cancer stem cells (OvCSCs): a novel approach for cancer therapy. *Int J Mol Sci*. 2018;19(3):710. doi:10.3390/ijms19030710
112. Sriram MI, Kanth SB, Kalishwaralal K, Gurunathan S. Antitumor activity of silver nanoparticles in Dalton's lymphoma ascites tumor model. *Int J Nanomedicine*. 2010;5:753–762. doi:10.2147/ijn.S11727
113. Zhang XF, Gurunathan S. Combination of salinomycin and silver nanoparticles enhances apoptosis and autophagy in human ovarian cancer cells: an effective anticancer therapy. *Int J Nanomedicine*. 2016;11:3655–3675. doi:10.2147/ijn.S111279
114. Gurunathan S, Jeyaraj M, Kang MH, Kim JH. Graphene oxide-platinum nanoparticle nanocomposites: a suitable biocompatible therapeutic agent for prostate cancer. *Polymers (Basel)*. 2019;11(4):733. doi:10.3390/polym11040733
115. Chaudhary P, Sharma R, Sahu M, Vishwanatha JK, Awasthi S, Awasthi YC. 4-Hydroxynonenal induces G2/M phase cell cycle arrest by activation of the ataxia telangiectasia mutated and Rad3-related protein (ATR)/checkpoint kinase 1 (Chk1) signaling pathway. *J Biol Chem*. 2013;288(28):20532–20546. doi:10.1074/jbc.M113.467662
116. Alarifi S, Ali D, Alkahtani S, Almeer RS. ROS-mediated apoptosis and genotoxicity induced by palladium nanoparticles in human skin malignant melanoma cells. *Oxid Med Cell Longev*. 2017;2017:8439098. doi:10.1155/2017/8439098
117. Di Guglielmo C, De Lapuente J, Porredon C, Ramos-López D, Sendra J, Borrás M. In vitro safety toxicology data for evaluation of gold nanoparticles-chronic cytotoxicity, genotoxicity and uptake. *J Nanosci Nanotechnol*. 2012;12(8):6185–6191. doi:10.1166/jnn.2012.6430
118. Meena R, Pal R, Pradhan S, Rani M, Rajamani P. Comparative study of TiO₂ and TiSiO₄ nanoparticles induced oxidative stress and apoptosis of HEK-293 cells. *Adv Mater Lett*. 2012;3:459–465. doi:10.5185/amlett.2012.icnano.157
119. Ibrahim F, Andre C, Iutzeler A, Guillaume YC. Analysis of the activation of acetylcholinesterase by carbon nanoparticles using a monolithic immobilized enzyme microreactor: role of the water molecules in the active site gorge. *J Enzyme Inhib Med Chem*. 2013;28(5):1010–1014. doi:10.3109/14756366.2012.705835
120. Zhang XJ, Greenberg DS. Acetylcholinesterase involvement in apoptosis. *Front Mol Neurosci*. 2012;5:40. doi:10.3389/fnmol.2012.00040
121. Park SE, Kim ND, Yoo YH. Acetylcholinesterase plays a pivotal role in apoptosome formation. *Cancer Res*. 2004;64(8):2652–2655. doi:10.1158/0008-5472.can-04-0649
122. Park SE, Jeong SH, Yee SB, et al. Interactions of acetylcholinesterase with caveolin-1 and subsequently with cytochrome c are required for apoptosome formation. *Carcinogenesis*. 2008;29(4):729–737. doi:10.1093/carcin/bgn036
123. Trajkovic K, Hsu C, Chiantia S, et al. Ceramide triggers budding of exosome vesicles into multivesicular endosomes. *Science*. 2008;319(5867):1244–1247. doi:10.1126/science.1153124
124. Kosaka N, Iguchi H, Hagiwara K, Yoshioka Y, Takeshita F, Ochiya T. Neutral sphingomyelinase 2 (nSMase2)-dependent exosomal transfer of angiogenic microRNAs regulate cancer cell metastasis. *J Biol Chem*. 2013;288(15):10849–10859. doi:10.1074/jbc.M112.446831
125. Claus RA, Bunck AC, Bockmeyer CL, et al. Role of increased sphingomyelinase activity in apoptosis and organ failure of patients with severe sepsis. *FASEB J*. 2005;19(12):1719–1721. doi:10.1096/fj.04-2842fje
126. Alessenko AV, Shupik MA, Gutner UA, et al. The relation between sphingomyelinase activity, lipid peroxide oxidation and NO-releasing in mice liver and brain. *FEBS Lett*. 2005;579(25):5571–5576. doi:10.1016/j.febslet.2005.08.085
127. Sinha S, Hoshino D, Hong NH, et al. Cortactin promotes exosome secretion by controlling branched actin dynamics. *J Cell Biol*. 2016;214(2):197–213. doi:10.1083/jcb.201601025
128. Parolini I, Federici C, Raggi C, et al. Microenvironmental pH is a key factor for exosome traffic in tumor cells. *J Biol Chem*. 2009;284(49):34211–34222. doi:10.1074/jbc.M109.041152
129. Lv LH, Wan YL, Lin Y, et al. Anticancer drugs cause release of exosomes with heat shock proteins from human hepatocellular carcinoma cells that elicit effective natural killer cell antitumor responses in vitro. *J Biol Chem*. 2012;287(19):15874–15885. doi:10.1074/jbc.M112.340588
130. Samuel P, Mulcahy LA, Furlong F, et al. Cisplatin induces the release of extracellular vesicles from ovarian cancer cells that can induce invasiveness and drug resistance in bystander cells. *Philos Trans R Soc Lond B Biol Sci*. 2018;373(1737):20170065. doi:10.1098/rstb.2017.0065
131. Eguchi A, Mulya A, Lazic M, et al. Microparticles release by adipocytes act as “find-me” signals to promote macrophage migration. *PLoS One*. 2015;10(4):e0123110. doi:10.1371/journal.pone.0123110
132. D'Souza-Schorey C, Clancy JW. Tumor-derived microvesicles: shedding light on novel microenvironment modulators and prospective cancer biomarkers. *Genes Dev*. 2012;26(12):1287–1299. doi:10.1101/gad.192351.112

133. Harmati M, Tarnai Z, Decsi G, et al. Stressors alter intercellular communication and exosome profile of nasopharyngeal carcinoma cells. *J Oral Pathol Med.* 2017;46(4):259–266. doi:10.1111/jop.12486
134. König L, Kasimir-Bauer S, Bittner AK, et al. Elevated levels of extracellular vesicles are associated with therapy failure and disease progression in breast cancer patients undergoing neoadjuvant chemotherapy. *Oncoimmunology.* 2017;7(1):e1376153. doi:10.1080/2162402x.2017.1376153
135. Osti D, Del Bene M, Rappa G, et al. Clinical significance of extracellular vesicles in plasma from glioblastoma patients. *Clin Cancer Res.* 2019;25(1):266–276. doi:10.1158/1078-0432.Ccr-18-1941
136. Keklikoglou I, Cianciaruso C, Güç E, et al. Chemotherapy elicits pro-metastatic extracellular vesicles in breast cancer models. *Nat Cell Biol.* 2019;21(2):190–202. doi:10.1038/s41556-018-0256-3
137. Kumar VA, Taylor NL, Shi S, Wickremasinghe NC, D'Souza RN, Hartgerink JD. Self-assembling multidomain peptides tailor biological responses through biphasic release. *Biomaterials.* 2015;52:71–78. doi:10.1016/j.biomaterials.2015.01.079
138. Herz F, Kaplan E. A review: human erythrocyte acetylcholinesterase. *Pediatr Res.* 1973;7(4):204–214. doi:10.1203/00006450-197304000-00024
139. Meshorer E, Yellajoshula D, George E, Scambler PJ, Brown DT, Misteli T. Hyperdynamic plasticity of chromatin proteins in pluripotent embryonic stem cells. *Dev Cell.* 2006;10(1):105–116. doi:10.1016/j.devcel.2005.10.017
140. Lutz HU, Liu SC, Palek J. Release of spectrin-free vesicles from human erythrocytes during ATP depletion. I. Characterization of spectrin-free vesicles. *J Cell Biol.* 1977;73(3):548–560. doi:10.1083/jcb.73.3.548
141. Pan BT, Blostein R, Johnstone RM. Loss of the transferrin receptor during the maturation of sheep reticulocytes in vitro. An immunological approach. *Biochem J.* 1983;210(1):37–47. doi:10.1042/bj2100037
142. Myrzakhanova M, Gambardella C, Falugi C, et al. Effects of nanosilver exposure on cholinesterase activities, CD41, and CDF/LIF-like expression in zebrafish (*Danio rerio*) larvae. *Biomed Res Int.* 2013;2013:205183. doi:10.1155/2013/205183
143. Yoshimura S, Banno Y, Nakashima S, et al. Inhibition of neutral sphingomyelinase activation and ceramide formation by glutathione in hypoxic PC12 cell death. *J Neurochem.* 1999;73(2):675–683. doi:10.1046/j.1471-4159.1999.0730675.x
144. Guo BB, Bellingham SA, Hill AF. The neutral sphingomyelinase pathway regulates packaging of the prion protein into exosomes. *J Biol Chem.* 2015;290(6):3455–3467. doi:10.1074/jbc.M114.605253
145. Back MJ, Ha HC, Fu Z, et al. Activation of neutral sphingomyelinase 2 by starvation induces cell-protective autophagy via an increase in Golgi-localized ceramide. *Cell Death Dis.* 2018;9(6):670. doi:10.1038/s41419-018-0709-4
146. Wu Z, He D, Li H. Bioglass enhances the production of exosomes and improves their capability of promoting vascularization. *Bioact Mater.* 2021;6(3):823–835. doi:10.1016/j.bioactmat.2020.09.011
147. Ilangumaran S, Ferbeyre G. Editorial: cytokines in inflammation, aging, cancer and obesity. *Cytokine.* 2016;82:1–3. doi:10.1016/j.cyt.2016.03.011
148. Barnes BJ, Somerville CC. Modulating cytokine production via select packaging and secretion from extracellular vesicles. *Front Immunol.* 2020;11:1040. doi:10.3389/fimmu.2020.01040
149. Bretz NP, Ridinger J, Rupp AK, et al. Body fluid exosomes promote secretion of inflammatory cytokines in monocytic cells via Toll-like receptor signaling. *J Biol Chem.* 2013;288(51):36691–36702. doi:10.1074/jbc.M113.512806
150. Valenti R, Huber V, Filipazzi P, et al. Human tumor-released microvesicles promote the differentiation of myeloid cells with transforming growth factor-beta-mediated suppressive activity on T lymphocytes. *Cancer Res.* 2006;66(18):9290–9298. doi:10.1158/0008-5472.Can-06-1819
151. McDonald MK, Tian Y, Qureshi RA, et al. Functional significance of macrophage-derived exosomes in inflammation and pain. *Pain.* 2014;155(8):1527–1539. doi:10.1016/j.pain.2014.04.029
152. Zhaogang yang Z, Shi J, Xie J, et al. Large-scale generation of functional mRNA-encapsulating exosomes via cellular nanoporation. *Nat Biomed Eng.* 2020;4(1):69–83. doi:10.1038/s41551-019-0485-1
153. Lu M, Huang Y. Bioinspired exosome-like therapeutics and delivery nanoplatforms. *Biomaterials.* 2020;242:119925. doi:10.1016/j.biomaterials.2020.119925
154. Liu H, Huang L, Mao M, Ding J. Viral protein-pseudotyped and siRNA-electroporated extracellular vesicles for cancer immunotherapy. *Adv Funct Mater.* 2020;30(52):2006515. doi:10.1002/adfm.202006515
155. Im E-J, Lee C-H, Moon P-G, et al. Sulfisoxazole inhibits the secretion of small extracellular vesicles by targeting the endothelin receptor A. *Nat Commun.* 2020;10:1387. doi:10.1038/s41467-019-09387-4

International Journal of Nanomedicine

Publish your work in this journal

The International Journal of Nanomedicine is an international, peer-reviewed journal focusing on the application of nanotechnology in diagnostics, therapeutics, and drug delivery systems throughout the biomedical field. This journal is indexed on PubMed Central, MedLine, CAS, SciSearch®, Current Contents®/Clinical Medicine,

Submit your manuscript here: <https://www.dovepress.com/international-journal-of-nanomedicine-journal>

Dovepress

Journal Citation Reports/Science Edition, EMBase, Scopus and the Elsevier Bibliographic databases. The manuscript management system is completely online and includes a very quick and fair peer-review system, which is all easy to use. Visit <http://www.dovepress.com/testimonials.php> to read real quotes from published authors.